S phase dependence and involvement of NF-kappaB activating kinase in NF-kappaB activation by Camptothecin

Yvette Habraken, Bernard Piret[1] and Jacques Piette[*].
Laboratory of Virology and Immunology, Institute of Pathology, B23, University of Liège, B-4000 Liège, Belgium.

* Corresponding author: Dr Jacques Piette, Laboratory of Virology & Immunology, University of Liège, Institute of Pathology B23, B4000 Liège, Belgium. Tel: + 32 4 366 24 42; Fax: + 32 4 366 24 33; Email: jpiette@ulg.ac.be.
[1] present address: B. Piret, Institute of Toxicology and Genetics, Forschungszentrum Karlsruhe, Hermann-von-Helmholtz-Platz 1, D-76344, Eggenstein-Leopoldshafen, Germany.

Abbreviations: ALLN, *N*-acetyl-leu-leu-norleucinal; AT, ataxia telangiectasia; CHX, cycloheximide; CPT, camptothecin; IκB, inhibitor kappa B; IKK, IκB kinase; MEKK1, mitogen-activated protein/ERK kinase kinase 1; NF-κB, nuclear factor kappa B; NIK, NF-κB inducing kinase; P-IκBα, phosphorylated IκBα, TNFα, tumor necrosis factor -α;

Abstract

Camptothecin (CPT) and derivatives are topoisomerase I poisons currently used as anticancer drugs. Their cytotoxicity is maximal for cells in S phase. Using asynchronous and S phase-synchronized HeLa cells, we have shown that both the nuclear factor-κB (NF-κB) activation and its transcriptional activity, induced by CPT treatment, are enhanced in S phase cells. After CPT treatment, NF-κB activation reaches a maximum in 2-3 hours and is still detectable after 24 hours. The nature of the complex evolves with time, forming mostly p50/p65 after 2 hours to almost exclusively p52 after 24 hours. In HeLa cells, the different steps of the induction are readily observable in S phase synchronized cells whereas they were difficultly noticeable in a randomly growing cell population. The signal progresses through the activation of the IKK complex, the phosphorylation of IκBα, the degradation of phosphorylated-IκBα and -IκBβ. The stable expression of wild-type HA-tagged-IκBα or mutated HA-tagged-IκBα (S32,36A) allowed us to confirm essential role of Ser32 and Ser36. NF-κB-activating kinase (NIK) could play a role upstream of the IKK complex as the transient expression of a kinase inactive mutant NIK(K429,430A) abolishes the activation of NF-κB by CPT. A kinase inactive mutant of mitogen-activated protein/ERK kinase kinase 1 (MEKK1) another kinase susceptible to act upstream of the signalsome does not. Cytotoxicity studies, with clonal populations expressing different amounts of wild-type or mutated IκBα, revealed that the overexpression of wild-type IκBα in large amount increases the sensitivity of HeLa cells to CPT more efficiently than a lower level of expression of non-phosphorylable IκBα.

Key words: camptothecin, NF-κB, S phase, signal transduction, DNA damage, NF-κB inducing kinase.

1. Introduction

Camptothecin (CPT) and derivatives are potent anticancer agents which inhibit DNA-topoisomerase I. The drug reversibly stabilizes the transient intermediate comprising DNA topoisomerase I covalently linked to the broken DNA strand, preventing the religation of the nick [1;2]. The CPT-topoI-DNA complexes (also called "cleavable complexes") can later be converted into lethal double-strand breaks by the replication machinery of the dividing cells [3-5]. Numerous studies have shown that actively dividing cells are more sensitive to CPT than non-dividing cells and that S-phase specific apoptosis can be detected in some cell types [6;7]. However, the precise way by which the cells attempt to deal with these double-strand breaks as well as the exact cell death pathway are yet undetermined. In addition to apoptosis, cell cycle arrests in G1, G2 and at internal S phase checkpoints are also observed following CPT-treatment [8;9]. Cells with an hypersensitivity to ionizing radiation or with abnormal cell cycle checkpoint in response to ionizing radiation, such as cells derived from individual suffering from ataxia telangiectasia (AT) or Nijmegen Breakage Syndrome, are more sensitive to CPT [10-12]. This enhanced sensitivity indicates the importance of post-DNA lesion processes.

Our laboratory and others reported that CPT activates the transcription factors NF-κB [13-15]. NF-κB belongs to a family of transcription factors composed of homo- or hetero-dimers of Rel proteins (p50, p65 (RelA), p52, RelB, c-Rel) which play an important role in the cellular response to stress. It is activated by many different extracellular stimuli among which pro-inflammatory cytokines (TNFα, IL1), bacterial lipopolysaccharides, phorbol esters, radiations (UV, X-rays), some viral proteins, ds-RNA, oxidative stress… [16-18]. Once activated, NF-κB modulates the expression of many genes involved in cellular events so diverse as inflammatory responses, cell growth and differentiation control, malignant transformation, and apoptosis [16;19-21]. A large body of literature comments on the anti-apoptotic function of NF-κB, but it is also evident that for some cell types and in some situations, NF-κB does not affect the cell faith or exhibits pro-apoptotic functions [21-23].

Currently, the best known activation pathway for NF-κB, is the cascade of events triggered by pro-inflammatory cytokines TNFα and IL1β [16;17;24]. In non-stimulated cells, NF-κB is maintained in the cytoplasm by a family of inhibitory proteins IκB (IκBα, IκBβ, IκBε, p100, p105). Upon stimulation by TNFα, IκBα is phosphorylated on two critical serine residues (S32 and S36) by the IKK complex, which itself needs to be activated by phosphorylation [25;26]. The phosphorylation of both serines 32 and 36 is the key step in regulating the multi-ubiquitination of phosphorylated-IκBα (P-IκBα) on two adjacent lysine residues (L21 and L22) and its subsequent degradation by the 26S proteasome. Free NF-κB then translocates into the nucleus where it binds to its target sequences. Though this system is the best studied, it is not the only possible route of activation. Other activation pathways independent of the IKK kinase complex were reported i.e. after oxidative stress or UV irradiation [18;27;28].

In this work, we studied the mechanism of activation of NF-κB by CPT. We present data indicating that CPT-induced NF-κB activation is mainly restricted to S phase. Although the kinetic of induction is different from the one observed with TNFα, the induction involves similar intermediates : (i) activation of the IKK complex, (ii) phosphorylation of IκBα on S32 and S36 and (iii) degradation of the phosphorylated-IκBα and -IκBβ, (iv) participation of the 26S proteasome. The involvement of two members of the MAP kinase family, NF-κB activating kinase (NIK) and the mitogen-activated protein kinase/ERK kinase kinase-1 (MEKK1) both able to directly interact with and activate the IKK complex, was also

investigated [29-36]. Using stably transfected HeLa cells overexpressing wild-type or mutated IκBα, we established that the S32, 36A mutations of the inhibitor are not necessarily sufficient to enhance the cytotoxicity of the drug. The wild-type IκBα can indeed be more effective if overexpressed to a higher level.

2. Materials and Methods

2.1. Chemicals and reagents

All enzymes and recombinant human TNFα were from Roche. Camptothecin (CPT), *N*-acetyl-leu-leu-norleucinal (ALLN), acetyl coenzyme A and cycloheximide (CHX) were purchased from Sigma, thymidine from Calbiochem. E64-d and *clastro*-lactacystin-β-lactone (lactacystin) were respectively obtained from Peptide International and Boston Biochemicals.

2.2. Plasmids

The plasmids expressing the inhibitors HA-IκBα and mutated HA-IκBα (S32,36A) under the control of the CMV promoter were obtained from Dr V. Bours (Laboratory Medical Chemistry from the University of Liège). HA-tagged MEKK1 wild-type and dominant negative (D1369A), c-myc-tagged NIK wild-type and dominant negative (K429,430A) all four under the control of the CMV promotor as well as pGST-IκBα$_{1-54}$ and pGST-IκBα$_{1-54}$ (S32,36A) expressing a fusion protein of GST and the 54 first amino-acid residues of IκBα either wild-type or mutated were kind gifts from Dr R. Gaynor (University of Texas Southwestern Medical Center). The κB-Luc reporter construct containing five κB sites from the HIV-1 long terminal repeat clone upstream of the Luciferase gene was from Stratagen and the expression plasmid containing the green fluorescent protein under the control of the CMV promotor from Clontech.

2.3. Cell culture

HeLa cells were grown in EMEM supplemented with 10% fetal calf serum at 37°C in a 5% CO_2 atmosphere. HeLa cells stably overexpressing HA-tagged IκBα either wild-type or mutated at both serines 32 and 36 (S32-36A) were obtained after transfection with the corresponding plasmids bearing a gene conferring resistance to geneticin G418. After 2 weeks, several clones were picked and screened for expression. A few selected clones positive for expression were subcloned.

The HeLa HIV-1 CAT cell line, expressing the bacterial *CAT* gene under the control of the long terminal repeat of the HIV-1, was received form K. Valerie (Virginia Commonwealth University, VI) and was cultivated in identical conditions to HeLa cells.

2.4. Synchronization of the cells

For G1/S synchronization, HeLa cells were grown for 18 hours in normal medium. The media was then replaced by fresh media containing 2 mM thymidine for 16 hours. After release in thymidine-free medium, the cells were grown for 10 hours, then exposed a second time to 2 mM thymidine for an additional 16 hours [37;38]. To monitor cell synchrony, the cells were collected at different times post-release of the block by trypsinisation, fixed in 70% (v/v) ethanol, stained with propidium iodide and analyzed by flow cytometry on a FACS Calibur (Becton Dickinson). The data were analyzed with the software WINMDI version 2.8.

2.5. Total, cytoplasmic and nuclear protein extracts.

All cells were plated the day preceding the experiment except when synchronized. Whole cell extracts were prepared by rapid lysis of the cells (grown in 6-well plates) in 300 µL of SDS-containing buffer (62.5 mM Tris-HCl pH 6.5, 2 % w/v SDS, 10 % glycerol, 25 mM DTT, 0.1 % bromophenol blue). The extracts were sonicated in a water bath for 40 seconds, boiled 2 min before centrifugation.

Cytoplasmic extracts and nuclear extracts were prepared as described earlier [18] except that 0.3 % (v/v) Igepal was added to the hypotonic buffer used to obtain the cytoplasmic extracts. Protein concentrations were determined with the Bio-Rad protein assay.

2.6. Western blotting

The presence of inhibitors (IκBα, IκBβ and IκBε) or phosphorylated-IκBα (P-IκBα) in total (20 - 40 µL) or cytoplasmic extracts (10 µg) was determined by immunoblotting using specific antibodies as described earlier [18]. Anti-IκBα monoclonal antibody was a gift from C. Dargemont (Curie Institute, Paris). Anti-phospho-IκBα-S32 antibody was purchased from New England Biolabs. The polyclonal anti IκBβ and IκBε antibodies were from Santa Cruz Biothechnology. The rat monoclonal antibody directed against the HA epitope was from Roche.

2.7. Electrophoretic Mobility Shift Assay (EMSA)

Binding reactions and supershift experiments were performed with 5 µg of nuclear proteins and 0.2 ng of [^{32}P] radiolabeled probe κB probe (5'- GGTTACAAGGGACTTTCC GCTG-3') [18]. The dried gels were autoradiographied and in some instances the amount of retarded probe was quantified by Phosphorimager analysis (Molecular Dynamics). When supershifts were performed, 5 µg nuclear proteins and 1 µg of antibody directed against either p50, p52, RelA, c-Rel, RelB (Santa Cruz Biotechnology) or phosphorylated-p38 (New England Biolabs) were incubated on ice for 20 min prior to the addition of the radioactive oligonucleotide probe. The complex protein/DNA was separated from the free probe on a 6% native polyacrylamide gel in the regular mobility assay and on a 4% native polyacrylamide gel in supershift assays. For the competition experiments, 10-, 50- or 100-fold molar excess of either wild-type or mutated probe (5'-GGTTACAACTCACTTTCCGCTG -3') were added to the incubation mixture.

2.8. CAT Assays

CAT activity was assayed as described by Neumann *et al.* [39]. This method is based on the solubility difference in a scintillation cocktail between the substrate of the reaction, [^{3}H] acetyl-coenzyme A, and the enzymatic product of the reaction, [^{3}H] acetyl-chloramphenicol. Only the product of the reaction diffuses in the organic phase where it can be detected. The CAT activity is given by the initial rate of the reaction. Three days prior to the drug treatment 1.3 x 10^5 cells were plated in 6 well tissue culture dishes. The next day, the synchronization process was initiated in half of the wells. CPT was added 4 hours post release of the second thymidine blockage and incubated for twelve hours. The cells were collected, washed in PBS, resuspended in 100 µL of 0.1 M Tris-HCl pH 7.8 and disrupted by three cycles of freezing and thawing. The extracts were centrifuged, the supernatants heated 15 min at 65°C and the denatured proteins precipitated. CAT activity was detected in the supernatant, 48 µL of supernatant was mixed to 198 µL of 1.25 mM chloramphenicol and 0.5 µCi [^{3}H]-acetyl coenzyme A (NEN Life Science Product) diluted with carrier acetyl CoA to 0.1 mM. The mixtures were overlaid with 5 mL EconoFluor (Packard) and the vials counted continuously in a liquid scintillation counter (Wallac) to generate kinetics of chloramphenicol acetylation.

2.9. Immunoprecipitation and *in vitro* kinase assay

Drug-treated and control HeLa cells were lysed in 10 mM HEPES-KOH pH 7.9, 3 mM EDTA, 10 mM KCl, 0.3 % (v/v) Igepal, 0.5 mM PMSF, 1 mM DTT, containing phosphatase inhibitors (1 mM NaF, 1 mM β-glycerophosphate, 1 mM Na_3VO_4, 1.5 mM *para*-nitrophenyl-

phosphate) and protease inhibitors (Complete® from Roche). After 20 min incubation on ice, the lysate was vortexed and centrifuged at 15000 *g*, for 5 min at 4°C. The supernatants containing the cytoplasmic proteins (250 µg) were then incubated 2 hours at 4°C with 1 µg anti-IKKα antibody in 50 mM Tris-HCl pH8.0, 250 mM NaCl, 3 mM EDTA, 3 mM EGTA, 0.1 % (v/v) Igepal plus all protease and phosphatase inhibitors described above. Finally 15 µL of protein A Sepharose beads (Pharmacia) were added and the incubation continued for a further 16 h at 4°C. The immunoprecipitates were washed 3 times in the incubation buffer and twice in kinase buffer containing 50 mM Tris–HCl pH 8.0, 100 mM NaCl, 2 mM DTT and the protease and phosphatase inhibitors. The immunoprecipitated proteins were then incubated with 0.5 µg GST-IκBα$_{1–54}$ or GST-IκBα$_{1-54}$ (S32,36A) and 10 µCi ATP-γ-[^{32}P] (ICN), in the kinase buffer for 30 min at 30°C. The reaction was stopped by addition of the Laemmli's sample buffer. The eluted proteins were subjected to a 12 % (w/v) SDS/PAGE. The gel stained by Coomassie blue to visualize the amount of substrate, was dried and autoradiographied.

2.10. Transient transfection assays

HeLa cells (3 x 10^5) were placed in 6 well-plates 24 hours prior to the transfection and grown in regular media. The transfections were effectuated with Fugene ^{6TM} (Roche) according to the manufacture procedures except that the ratio (µL FUGENE/ µg ADN) was 2.5 instead of 3. Cells were transfected with 100 ng of plasmid bearing the κB-LUC insert and increasing amount of plasmid expressing the kinase inactive mutant of NIK or MEKK1. Six hours and a half after transformation, the media was replaced and the cells treated with TNFα (200 U) or CPT (3 µM) for 12 hours. The cells were then washed in PBS, scraped, lysed for 15 min at room temperature, and centrifuged at 15000 x g for 10 min at 4°C. The Luciferase activity of the supernatant was measured with the Luciferase Reporter Kit from Roche. The values obtained were corrected for the amount of protein.

2.11. Determination of cellular viability

Stably transformed cells were seeded at the concentration of 3000 cells par well in flat-bottomed 96 well plates and cultivated with 0.2 mL medium. The cells were grown for 24 hours without geneticin G418, then the media was removed and fresh media containing appropriated concentrations of CPT was added. After 48 hours of incubation with the drug; cell viability was measured by a colorimetric assay based on the cleavage of the tetrazolium salt WST-1 by mitochondrial dehydrogenase in viable cells (Roche).

3. Results

3.1. NF-κB DNA binding activity induced by CPT

To study NF-κB activation by CPT, we examined the induction of NF-κB DNA binding activity in nuclear protein extracts by EMSA. Exponentially growing HeLa cells were treated with a single dose of TNFα (200 U/ mL) or CPT (10 μM) for increasing period of time. This CPT concentration is compatible with the plasma concentrations observed immedialy after the injection of the compound (7.7μM for Irinotecan a soluble analog of CPT in human and 5.8 μM for CPT in mice) [Rhône Poulenc Rhorer and [40]]. The cells were kept in contact of the drugs for the entire duration of the incubation. Contrarily to the rapid NF-κB induction observed after addition of TNFα [25;41] (Fig. 1A, lanes 1-6, top panel), the CPT-induced NF-κB binding activity was much slower and more stable (Fig. 1A, lanes 7-14, top panel). NF-κB response elicited by TNFα was maximal after 20 min, sustained for 1 hour, then began to decline; whereas NF-κB was first detected one hour after exposure to CPT and increased steadily until it reached a maximum after about 2-3 hours. The induction was maintained for many hours and was still detectable after 24 hours (Fig. 1A, lane 14). The activation of NF-κB by CPT is observed with concentration of CPT as low as 0.1μM and increases as the drug concentration is augmented (data not shown and Fig. 1B in ref. 13).

The specificity of the DNA/protein complexes formed two hours after the addition of CPT was ascertained by competition assay (Fig. 1B). The slower migrating complex was efficiently competed away by as little as a 10-fold excess of the unlabelled κB probe and completely abolished by a 50-fold or 100-fold excess but not by the same excess of an unlabeled mutated κB oligonucleotide. The faster migrating complex was unaffected by either probes.

As the CPT-induced activation of NF-κB is slow in regard of the cellular response produced by TNFα, the induction pathway of NF-κB used by CPT could have required the synthesis of *de novo* proteins. But as already reported earlier in other cell types CEM and 70Z/3 [13;15], the incubation of HeLa cells for 30 min with cycloheximide (CHX) a traduction inhibitor, prior to CPT addition, did not modify the intensity of the DNA/protein complex indicating that no protein synthesis is required. Under these conditions, the CHX did not activate NF-κB neither did it modify the level of IκBα (data not shown).

The long lasting induction of NF-κB incited us to compare the nature of the specific protein/DNA complex obtained 6 hours after CPT addition, with the composition of the complex formed after 2 hours and 24 hours. After 6 hours, the specific complex contained mostly p65 (RelA), p50 and p52 as the apparition of supershifted bands correlated with a partial depletion of this complex (Fig. 1C, lanes 2, 3 and 4). A supershifted band was also detected using anti-c-Rel antibodies but without apparent diminution of the specific complex indicating that c-Rel is a minor component (Fig. 1C, lane 5). No supershifted bands were detected either with anti-RelB antibody or the non-related anti-phosphorylated-p38 antibody (Fig. 1C, lanes 6, 7). After 2 hours, the complex had a similar composition but with a smaller representation of p52 (data not shown) and was thus mostly constituted of p50 and p65. After 24 hours, the nature of the complex was different, p52 being the predominant species present (Fig. 1C, lane 11). The relative amount of p50, p65 and c-Rel supershifted decreased (Fig. 1C, lanes 9, 10, 12) and the complex was disrupted by anti-RelB antibody indicating the presence of RelB (Fig. 1C, lanes 13). Thus the complex composition evolved with time. At first, the heterodimer p50/p65 is the major subset represented then is substituted by p52 and RelB.

3.2. S phase dependence of the activation of NF-κB by CPT

As the cytotoxic effect of CPT is maximal for S phase cells [4], we compared the NF-κB induction in a randomly growing population and in synchronized cells. HeLa cells were synchronized by forcing an arrest at the G1/S border by exposition to an excess thymidine. Four hours after the release of the block, a majority of HeLa cells were in S phase of the cell cycle as confirmed by FACS analysis (Fig. 2A). The proportion of cells in G1, S and G2 were respectively of 62%, 11%, 22% in the random population and of 15%, 55% and 21% in the synchronized population. A direct comparison between the signal detected in S phase or randomly growing cells, 4 hours after the addition of CPT, revealed that NF-κB activation, measured by the radioactivity associated with the specific complex, was 4 fold more important in the synchronized cells (Fig.2B, lanes 2 and 4). The procedure of synchronization did not elevate the basal level of NF-κB significantly (Fig. 2B; lanes 1 and 3). The kinetic of induction of NF-κB in S phase synchronized cells was similar to the one observed in randomly growing cells (Fig. 2C and 2D top panels). NF-κB binding activity was still slow to appear (Fig. 2C, top panel) and stable for many hours (Fig. 2D, top panel).

In order to see whether the enhanced NF-κB induction observed in S phase cells was reflected at the transcriptional level, we used the HeLa HIV-1 CAT cell line. In this cell line, the bacterial *CAT* gene with a polyadenylation signal was placed under the control of the HIV-1 long terminal repeat. Three days prior to the drug treatment 1.3×10^5 cells were placed in 6 well tissue culture dishes. The next day, the synchronization process was initiated in half of the wells. Four hours after the release from the thymidine blockage, CPT (3.3 µM) was added and incubated for 12 hours. At the end of the incubation period, the level of CAT activity present in the cells was measured. As shown in Fig. 2E, representing the initial rates of release of [^{3}H] acetyl-chloramphenicol, the NF-κB induced by CPT is transcriptionally active as the level of CAT activity increased in response to CPT (compare triangle to square symbols). For an identical CPT concentration (3.3 µM), there is a 2.2 fold stimulation of the CAT activity induced when the cells are in S phase. Under these experimental conditions, the values of the initial rate of reaction calculated between 66 and 102 min were of 636 cpm/min and 288 cpm/min for the CPT treated S phase cells or randomly growing cells respectively. In control cells, exempt from CPT treatment, the basal level of CAT activity was not affected by the synchronization process (compare closed and open square).

3.3. Time course of CPT-induced degradation of the IκB family members

In a first time, the level of cytoplasmic IκBα was followed in extracts from asynchronous HeLa cells, treated either with TNFα or CPT for increasing periods of time (Fig. 1A, bottom panel). As already described by others [25;41] TNFα (200 U/ mL) induced a rapid and transient degradation of IκBα (Fig. 1A, bottom panel, lanes 1-6). The level of degradation of IκBα following CPT treatment was much weaker and in some experiments not detected at all (Fig. 1A, bottom panel, lanes 7-14). In a second time, cytoplasmic extracts from mostly S phase cells treated with CPT were analyzed for their content in IκBα up to three hours after addition of CPT (Fig. 2C, bottom panel) or for longer lengths of time (Fig. 2D, second panel).

Under these conditions, the depletion of cytoplasmic IκBα is almost complete and long lasting. Thus, the level of degradation of IκBα is more pronounced for cells in S phase than for random cells. The re-synthesis IκBα is observed about 6 hours after CPT addition, this re-synthesis precedes of many hours the disappearance of NF-κB induction. This is why, we also examined the level of two other inhibitors IκBβ and IκBε in cytoplasmic extracts (Fig. 2D, two bottom panels). IκBβ is degraded too, though to a lesser extent than IκBα. The inhibitor

IκBε does not seem to be degraded. Its level detected 24 hours after the addition of CPT is in fact higher that at the beginning of the reaction.

3.4. CPT-induced phosphorylation of IκBα

In order to determine whether the signal transduction initiated by CPT has other common steps with the cascade of events initiated by TNFα, we monitored the phosphorylation of the serine 32 of IκBα. The presence of phosphorylated IκBα (P-IκBα) was followed in total cellular extracts by Western blotting with a polyclonal antibody raised specifically against IκBα posphorylated on serine 32. S phase cells were treated with TNFα (1000 U/ mL) or CPT (10 µM) for the indicated time (Fig. 3A). P-IκBα was detected both in response to TNFα and CPT. The time course of apparition and the quantity formed are however quite different. After TNFα treatment, P-IκBα is rapidly (5 min) and transiently detected. Fifteen min after the addition of TNFα the amount of P-IκBα is already decreasing. After CPT treatment, the generation of P-IκBα is slower, none is detected after 30 min, its level is maximal after 60 min and then decreased. Its presence is still detectable at 90 min. Phosphorylated IκBα was undetectable in a randomly growing cell population (data not shown). The apparition of P-IκBα is preceding the NF-κB induction. It is maximal 60 min after CPT addition whereas NF-κB activation reaches a maximum after 2, 3 hours.

3.5. Activation of the endogenous IKK by CPT

Endogenous IKK kinase activity was monitored following immunoprecipitation with an anti-IKKα antibody that precipitated the IKKα /IKKβ / IKKγ complex. Cytoplasmic extracts from S phase synchronized cells treated either with TNFα or CPT were tested. The immunoprecipitated proteins were incubated with GST-IκBα $_{1-54}$ or its mutated version in presence of ATP-γ-[^{32}P]. A strong activation of the IKK kinase by TNFα was detected after a very short time (Fig. 3B, top panel lanes 5, 6) [29;41]. Whereas the CPT–related activation of the IKK was much weaker. The kinase activation was sustained for as long as two hours (Fig. 3B, top panel, lanes 1-4). Once again, we could not detect any activation of the IKK complex in a randomly growing cell population (data not shown). Although the level of P-IκBα was maximal 60 min post CPT-addition (Fig. 3A) and weaker after 90 min, the level of activation of the IKK is stable at least for 2 hours. It could reflect an equilibrium between a stable activation of the IKK kinases by CPT and an increasingly efficient degradation of P-IκBα or a deficit in IκBα. The CPT-induced phosphorylation of IκBα seemed to be classically targeted on S32 and S36, no incorporation of radioactivity was detected on the mutated GST-IκBα$_{1-52}$ (S32,36A) (Fig. 3B bottom panels).

3.7. Requirement of S32 and S36 in the CPT-induced degradation of IκBα

In order to make certain IκBα degradation relies on S32 and S36, we generated HeLa cells stably expressing an epitope tagged HA-IκBα or its mutated form HA-IκBα (S32,36A). A control population of HeLa cells stably transfected with the empty vector was also established. Four clones expressing either low or high level of the inhibitor were selected and subsequently sub-cloned (Fig. 4A). Both CPT-related NF-κB DNA binding activity and IκBα degradation were studied on these clones.

At low level expression, the exogenous HA-IκBα did not modify the NF-κB induction, the same activation was observed in these cells and in the control cells expressing no HA-IκBα (Fig. 4B, upper panel, lanes 1-5 and 6-10). On the opposite, in the clonal population expressing a very large quantity of HA-IκBα, NF-κB induction was completely abolished (Fig. 4B, upper panel, lanes 11-15). In these cells, both TNFα- and CPT- induced responses

were totally repressed. Similar results were obtained with the clones expressing mutated HA-IκBα (S32,36A). At low level expression, the mutated IκBα did not alter the induction of NF-κB (Fig. 4B, lower panel, compare lanes 1-5 to lanes 6-10) whereas the binding activity was partially repressed in the clone expressing high level of mutated HA-IκBα (Fig. 4B, lower panel, lanes 11-15). In this case, the signal was not completely abolished because of the lesser level of expression of the HA-IκBα (S32,36A) (Fig. 4B, lanes 2 and 4).

The CPT-induced degradation of wild-type HA-IκBα can be seen in both low and high level expressing clones (Fig. 4C, top panels). The level of HA-IκBα steadily decreased with time over the period tested, no accumulation of the phosphorylated form was noticeable suggesting that the ubiquitination and degradation machinery is able to process P-HA-IκBα as it appears. The slower mobility form of HA-IκBα corresponding to the phosphorylated HA-IκBα is apparent following TNFα treatment. Its presence indicates - i) that the exogenous HA-IκBα is efficiently recognized and phosphorylated by the kinase – ii) that the proteasome is unable to degrade the P-IκBα as quickly as it is generated. The apparent lack of HA-IκBα degradation in the high level expression clone may be explained by the very high level of expression of the inhibitor, its degradation by the 26S proteasome may go unnoticed if it corresponds to the degradation of a small fraction of the HA-IκBα.

The analysis of both clones expressing low and high level mutated HA-IκBα (S32,36A) indicated that the mutated inhibitor was resistant to the degradation induced by TNFα as well as by CPT. The data presented above confirmed that CPT-induced degradation of IκBα requires the presence of S32 and/ or S36.

3.8. Involvement of the 26S proteasome in the signal transduction

It is well known that the 26S proteasome is responsible (only partially in some cell types) of the degradation of P-IκBα after TNFα treatment [42]. To verify the role of the 26S proteasome in the CPT-related degradation of IκBα, we first used ALLN. This tripeptide aldehyde is known to inhibit the 26S proteasome, calpain and cathepsin B [43;44] and was employed with success to stabilize P-IκBα after different stimuli such as TNFα and UV [27]. In the following experiments, HeLa cells were or were not pre-incubated 45 min with ALLN prior to the incubation with TNFα or CPT. As can be seen in Fig. 5A (lanes 5, 6), the ALLN pre-treatment has a very strong effect on the CPT related NF-κB activation. The diminution of the NF-κB induction in response to CPT is even more pronounced that the decrease observed in the TNFα treated cells (lanes 2, 3). The stabilization of P-IκBα was monitored in cytoplasmic extracts of S phase cells (pretreated or not). As can be seen on the top panel of Fig. 5B, the ALLN pre-treatment stabilized the phosphorylated forms of IκBα both after TNFα and CPT treatments (compare lanes 2 with 3 and 5 with 6). Two slow migrating bands are stabilized in the ALLN/TNFα treated cells (lane 3), they could represent the successive phosphorylation of the two serines

As already mentioned earlier in this paragraph, ALLN is not a specific inhibitor of the 26S proteasome. Thus, in order to study more precisely the events observed we used two different specific inhibitors: lactacystin (specific of the 26S proteasome) and E64-d (specific for calpain). S phase synchronized cells were pre-incubated or not with one of these inhibitors 45 min prior to TNFα or CPT addition and the level of P-IκBα was monitored in total cellular extracts. The stabilization of P-IκBα was detected in Lactacystin/TNF-treated cells (Fig. 5B, middle panel, lanes 2-4) and in Lactacystin/CPT treated cells (lanes 5 and 6). The calpain inhibitor, E64-d, did not seem to have any effect (Fig. 5B, bottom panel).

3.9. Inhibition of CPT-induced NF-κB activation by kinase deficient NIK

Next, the involvement of NIK in the cascade of events between the CPT induced DNA damage and the activation of NF-κB was investigated. NIK was originally identified as a TRAF2 interacting protein. It interacts strongly with IKKα [29-30]. When overexpressed, NIK constitutively activates NF-κB whereas kinase inactive mutant of NIK blocks NF-κB activation by TNFα [31-35].

Exponentially growing HeLa cells were co-transfected with the κB-Luc expression vector and increasing amount of a kinase deficient NIK mutant (K429,430A), then subsequently treated with TNFα (200 U/ mL) or CPT (3 µM). The Luciferase activity was measured in total cellular extracts prepared 12 hours after the addition of the drugs. As can be seen on Fig. 6A, the activation of NF-κB by CPT was efficiently blocked by this kinase deficient NIK. Moreover, this inhibition is dose dependent. It suggests that NIK is required for the CPT induced NF-κB activation. As expected, the NF-κB activation elicited by TNFα is also blocked.

The effect of kinase deficient MEKK1 was evaluated in a similar manner. In this case, however the CPT elicited activation of NF-κB was not inhibited, the level of Luc activity remained more or less constant, a slight activation was observed (Fig.6B).

The interference of mutated NIK on the activation of the IKK by CPT was also examined. HeLa cells were synchronized and transfected with a high amount of either mutated MEKK1 or mutated NIK or with a carrier vector. The transfection efficiency was monitored by fluorescence. Under the conditions used, 50% of HeLa cells, transfected with a plasmid expressing the fluorescent green protein were fluorescing 24 hours after the transfection. Twenty-four hours after the transfection, the transfected cells were treated with CPT (10 µM) for 80 min and the kinase activity was detected in the fraction of proteins immunoprecipitated by anti-IKKα antibodies. As shown in Fig. 6C, the level of activation of the IKK was decreased in the cells expressing mutated NIK. The amount of radioactivity present in each spot was quantified by phosphorimaging analysis. If an arbitrary value of 100 is given to the amount of radioactivity incorporated in GST-IκBα by the extract derived from the CPT treated cells, that amount drops to 52 for the cells expressing mutated NIK.

3.10. Cytotoxicity of CPT

To determine whether the overexpression of IκBα or mutated IκBα influences the cytotoxicity of CPT, we measured the viability of these cells after 48 hours exposition to different CPT concentration (0.1 µM- 1 µM). A low expression level of wild-type IκBα did not significantly affect the cellular resistance to CPT whereas large overexpression of the inhibitor markedly increased its sensibility (Fig. 7A). At 0.1 µM the survival of the cells expressing only the endogenous IκBα was 72%, whereas the cells expressing low level of exogenous IκBα or the high level had a survival rate of 77% and 11% respectively. The expression of either low or high level of mutated IκBα had a minor negative effect on the survival (Fig. 7B). At 0.6 µM, the cells overexpressing a large quantity of mutated IκBα had a survival rate of 24% whereas the cells non expressing any, exhibited a survival rate of 42%.

4. Discussion

The goal of this study was to determine the intermediate steps of the activation of NF-κB following CPT-induced DNA damage and to further define the kinetics of these steps. As the sole target of this drug is DNA-topoisomerase I, the nature of the initial damage is well defined and limited to DNA single- and double-strand breaks. The resulting signal transduction could have been entirely different of the one observed with the cytokine TNFα, which originates at the level of the membrane receptor TNF-R1. However, it was shown that, thought the signal does not originate from the same cellular compartment and though the kinetic of NF-κB inductions is different, both signaling cascades share common intermediates. The activation of the IKK complex, the phosphorylation of the inhibitor IκBα on S32 and S36 and its subsequent degradation, and the participation of the 26S proteasome are observed in both signal transductions. This indicates that, early in the transduction cascade elicited by CPT, a signal transfers from the nuclei into the cytosol. Another study reached the same conclusion [15]. Ionizing radiation, generating double-strand breaks, induce NF-κB in a rather similar manner than CPT. The IR-induced NF-κB activation is also slow and rely on the phosphorylation of both S32 and S36 of IκBα as well as the participation of the 26S proteasome [27].

By supershifting the protein/DNA specific complex with antibodies, we have shown that CPT treatment activated multiple NF-κB DNA binding complexes, and that the nature of these complexes evolved with time. At first, after two hours, mostly p50 and p65 were present with p52 and c-Rel in little amount; the heterodimers formed were very likely the same as those identified after TNFα induction in HeLa cells (p50/p65, p52/p65, p50/c-Rel and p52/c-Rel) [45]. IκBα being principally complexed to the p50/p65 heterodimer in the cytosol, its degradation will lead to the transfer of this specific heterodimer in the nuclei. Then, as time goes, we observed more and more p52 and the apparition of RelB. This sequential evolution of the complex was likely to result from the subsequent degradation of the other IκB inhibitors. As the nature of the dimers dictates its affinity to the consensus κB sequences, the induction of different subsets of the Rel family modifies the target genes [46-48]. It was noted that IκBα resynthesis preceded of many hours the inactivation of NF-κB. IκBβ whose degradation is less pronounced but long lasting is probably responsible for the late NF-κB activation. In resting cells, IκBβ and ε are associated with large amount of RelA and c-Rel [49]. We could not detect any substential degradation of IκBε. IκBε however was inducible by CPT treatment as it level was more elevated 24 hours after the addition of the drug than in the control cells.

One principal characteristic of CPT is its cytotoxicity specifically associated with the S phase of the cell cycle. The consensus in the literature was that lethal double-strand breaks are created by the collision of the replicative machinery with cleavable complexes, thus concentrating the formation of these lethal lesions in S phase. But a recent study seems to indicate that the number of double-strand breaks is not the only decisive factor, that in fact the post DNA damage pathway activated by the cells could be different in S phase than in other phases of the cell cycle [50]. Studies with AT cells, where the kinetic of NF-κB activation following CPT treatment is modified, also indicated the importance of these post DNA damage events [14]. This hypothesis might be further reinforced by a recent observation indicating that, following ionizing radiation, ATM phosphorylated nibrin (the protein deficient in the Nijmegen Breakage Syndrome) at an S-phase internal check-point [51]; thus, confirming the existence of a S phase specific event in the cellular response to double strand breaks. In this work, we have shown that the CPT-induced NF-κB activation is principally initiated during the S phase. The NF-κB induction (detected by EMSA) is enhanced four times

in S phase synchronized cells by comparison with a randomly growing population. The NF-κB transcriptional activity induced by CPT (detected by CAT assay) is stimulated 2.2-fold in S phase synchronized cells. This lack of proportionality between NF-κB activation and its transcriptional activity could be due to the difference in the length of time between the addition of the drug and the preparation of the extracts in the two different assays. Other arguments confirmed the S phase dependence: i) the activation of the IKK kinases is stronger, ii) higher quantity of P-IκBα are detected and iii) the degradation of IκBα (hardly observable in a non-synchronized population) is almost complete when cells are in S phase. The lag between CPT addition and NF-κB apparition in the nuclear extracts is not reduced in S phase cells, indicating that the NF-κB induction detected in the random population reflects what happens in S phase.

In general, the ubiquitin proteasome pathway plays an important role in two aspects of the NF-κB activation. It participates to the generation of p50 and p52 subunits, which are principally generated by a co-translational proteolytic processing, and it degrades ubiquitinated phosphorylated IκBα, β and ε [52-54]. We observed that ALLN and lactacystin stabilized P-IκBα after TNF and CPT treatment. In the signal transduction specific to CPT, the proteasome could yet act at additional levels. Indeed, it was reported that 10 min post CPT addition, 10% of the DNA-topoisomerase I involved in the cleavable complexes was multi-ubiquitinated and then degraded by the proteasome [55;56]. This degradation could be a crucial step of the signal transduction. However, the ubiquitination of the topoisomerase I trapped in the cleavage complex was recently challenged. Other authors reported that CPT induces a rapid and extensive conjugation of SUMO-1 to DNA topoisomerase I and that proteases different from the 26S proteasome are involved in this pathway [57]. In a recent publication it was shown that the cellular response to a proteasome inhibitor treatment associated to CPT was different if the inhibitor treatment preceded the CPT addition or if it followed it [58]. And finally, it has to be kept in mind that the proteasome also participates in cell cycle progression and could also interferes with the CPT-induced NF-κB activation by blocking the cell in a non reactional phase [59;60].

The activation of the IKK complex is presently under intensive scrutiny. Either upstream activating kinases are necessary or IKK, stimulated by the transient association with other partners in a multiprotein complex, autophosphorylates and autoactivates. Based upon the studies involving overexpression of recombinant proteins, two kinases MEKK1 and NIK have been shown to interact with and to activate the IKK complex. Using dominant negative NIK and MEKK1, we studied the effect of these two mutated kinases on the CPT induced NF-κB activation. Only the overexpression of NIK (K429,439A) negatively regulated the activation of NF-κB ; thus indicating the participation of NIK in the signaling cascade. The reduced level of activation of IKK, monitored in a kinase assay, confirmed the negative interference of mutated NIK in the CPT-induced signaling cascade. Activated NIK could interact with other proteins i.e. (receptor interacting protein) RIP with the IKK [61].

Finally, we observed that the ectopic overexpression of wild-type IκBα can have a stronger influence on the survival rate of the cells, than the overexpression of the mutated inhibitor. In the clone expressing HA-IκBα 10- to 15- fold over the level of the endogenous IκBα, the induction of NF-κB was completely abolished after both TNFα and CPT treatments. It indicates that the prevention of NF-κB activation can be achieved very efficiently by overwhelming the degradation capacity of the proteasome and that, in HeLa cells, NF-κB exhibits a classical anti-apoptotic function following CPT treatment.

Our results contribute to a better understanding of the few steps immediately preceding the activation of NF-κB in the cascade of events initiated by CPT related DNA damage. The exact nature of the S phase specific step leading to the activation of the IKK, as well as the nature of the signal leaving the nuclei are still under investigation. The precise knowledge of every steps implicated in this signal transduction would bring valuable information for the development of new drugs interfering with the activation of NF-κB or new anticancer drug.

Aknowledgements

We thank Dr R. Gaynor from the University of Texas Southwestern Medical Center at Dallas for the kind gift of the plasmids GST-IκBα$_{1-54}$ wild-type and mutated on S32 and S36 and for the plasmids expressing NIK and MEKK1. We are grateful to Dr V. Bours (Laboratory of Medical Chemistry, University of Liège) who supplied us with the plasmids overexpressing HA-IκB-α wild-type or mutated. We are also very much in debt to Dr Olivier Jolois (Laboratory of Histology, University of Liège) who performed the FACS analyses and to Dr K. Valerie (Virginia Commonwealth University, VI) for the gift of the HeLa–HIV-1 CAT cell line.

This work was supported in part by grants from the National Belgian Fund for Scientific Research (NFSR, Brussels, Belgium), from the Concerted Action Program (University of Liège) and by a starting up grant from the University of Liège.

Figure Legends

Fig. 1. *Activation of NF-κB and degradation of IκBα elicited by TNFα or CPT in HeLa cells.*
A) *Upper panel: NF-κB DNA binding activity.*
5 µg of nuclear extracts derived from exponentially growing HeLa cells, non-treated (lanes 1 and 7), treated with TNFα (200 U/ mL) (lanes 2-6) or treated with CPT (10 µM) (lanes 8-14) for the indicated length of time were tested for their ability to retard a [^{32}P]-radiolabeled oligonucleotide (0.2 ng) containing the κB consensus sequence. Migrating position of the specific NF-κB/DNA complexes (sp) and non-specific protein/DNA complex (nsp) are indicated.
Bottom Panel: Stability of IκBα.
Cytoplasmic extracts derived from the same cells were analyzed for their content in IκBα. Proteins (10 µg) were separated on a 10 % polyacrylamide gel and immunoblotted with anti-IκBα antibodies. Lanes 1 and 7: non-treated cells; lanes 2-6: cells treated by TNFα for 10, 20, 40, 60, 120 min; lanes 8-14: cells treated by CPT for 30, 60, 120, 180, 240, 360 min and 24 hrs. The position of IκBα is indicated.
B) *Specificity of the NF-κB complexes induced by CPT.*
Nuclear extracts prepared from HeLa cells treated 2 hours with CPT (10 µM) were incubated with the [^{32}P] radiolabeled probe in the usual conditions (lane 1), with a 10-, 50-, 100- fold excess of the unlabeled wild-type κB probe (lanes 2-4) or with a 10-, 50-, 100- fold excess of an unlabeled κB mutated probe (lanes 5-7).
C) *Nature of the NF-κB complexes induced by CPT.*
Nuclear extracts from HeLa cells, treated 6 hours (lanes 1-7) or 24 hours (lanes 8-14) with CPT 10 µM, were incubated for 15 min on ice in the binding buffer alone (lanes 1 and 8) or with antibodies directed against p50 (lanes 2 and 9), p65 (RelA) (lanes 3 and 10), p52 (lanes 4 and 11), c-Rel (lanes 5 and 12) and RelB (lanes 6 and 13) or phosphorylated p38 (lanes 7 and 14). After that time, the [^{32}P] oligonucleotide probe was added and the incubation continued at room temperature for an additional 30 min. The specific complexes and the supershifted bands are respectively indicated by sp and a bracket.

Fig. 2. *S phase dependence in NF-κB activation by CPT.*
A) *FACS analysis of asynchronous or synchronized cell populations.*
Exponentially growing HeLa cells asynchronous (left panel) or synchronized (right panel) were trypsinized, fixed, stained with propidium iodide and analyzed by FACS for relative DNA content. The synchronized cells were collected 4 hours post release of the thymidine block. The position of the peaks G1, S and G2 are indicated.
B) *Comparison of the NF-κB activation in randomly growing cells and S phase cells.*
Nuclear extracts derived from asynchronous (lanes 1, 2) or S phase synchronized (lanes 3, 4) cells treated 4 hours with CPT (10 µM) (lanes 2 and 4) were tested by EMSA.
C) *Activation of NF-κB and degradation of IκBα by CPT in S phase cells.*
Upper panels: NF-κB DNA binding activity.
Four hours post-release of the thymidine block, CPT (10 µM) was added to the S phase synchronized cells. At the indicated time after CPT addition, nuclear extracts were prepared and the NF-κB DNA binding activity was determined by EMSA. The migrating position of the specific NF-κB/DNA complexes (sp) and non-specific protein/DNA complex (nsp) are indicated.
Lower panels: IκBα degradation induced by CPT in S phase cells.

For the detection of IκBα, 10 µg of cytoplasmic extracts, prepared from the same S phase synchronized cells, were analyzed by immunoblotting with anti-IκBα antibodies. Extracts from non-treated control cells are in lane 1.

D) *Long term CPT-induced activation of NF-κB and degradation of IκB in S phase cells*

Upper panels: NF-κB DNA binding activity.

As reported in Fig. 2C over a longer length of time.

Lower panels: IκB degradation induced by CPT in S phase cells.

IκBα, IκBβ and IκBε were detected in 10 µg of cytoplasmic extracts, prepared from the same S phase synchronized cells, by immunoblotting with anti-IκBα, -IκBβ or -IκBγ antibodies. Extracts from non-treated control cells are in lane 1.

E) *Transcriptional activity of NF-κB in randomly growing cells or S phase synchronized cells*.

HeLa HIV-1 CAT cells were plated in 6 well tissue dishes and synchronized or not. Four hours after the release of the thymidine block, both cell populations were treated for 12 hours with CPT (3.3 µM) or not. The CAT activity was measured in total extracts prepared from asynchronous (open symbols) or S phase (closed symbols) HeLa HIV-1 CAT cells. CPT treated cells are represented by triangles, control cells by squares.

Fig. 3. *CPT induces the phosphorylation of IκBα by the IKK*.

A) *CPT induces the phosphorylation of IκBα*.

Total cellular extracts were prepared from S phase HeLa cells incubated 5, 10, 15 min with 1000 U/ mL of TNFα (lane 2-4) or 30, 60, 90 and 120 min with CPT 10 µM (lanes 5-8). Extracts from non-treated cells are in lane 1. The presence of P-IκBα was monitored with an antibody directed against IκBα–phosphorylated on S32. CPT was added to the synchronized cells 4 hours after the release of the thymidine block. The positions of P-IκBα and from a non specific (ns) band are indicated.

B) *Endogenous IKK kinases are activated by CPT*.

S phase synchronized cells were either non-treated (lane 1), treated with CPT (10 µM) for 40, 80, 120 min (lanes 2-4) or with TNFα (1000 U/ mL) for 5 and 7 min (lanes 5 and 6). After treatment, cytoplasmic extracts were prepared and immunoprecipitated with an anti-IKKα antibody. The IKK kinase activity in the immunoprecipitated proteins was assayed on either the wild-type GST-IκBα $_{1\text{-}54}$ (upper panel) or mutant GST-IκBα$_{1\text{-}54}$(S32,36A) (lower panel).

Fig. 4. *Serines 32 and 36 of IκBα are essential for CPT induced degradation***.**

A) *Stable overexpression of HA-IκBα or mutated HA-IκBα (S32,36A) in HeLa cells*.

Cytoplasmic extracts (10 µg) were analyzed by immunoblotting. Lane 1, HeLa cells transfected with the control vector; lanes 2 and 3, two selected clones expressing different amounts of mutated HA-IκBα (S32,36A); lanes 4 and 5, two selected clones expressing different amounts of exogenous HA-IκBα.

B) *Overexpression of wild-type or mutated IκBα modifies the induction of the NF-κB.*

Upper panel: Nuclear extracts from clonal populations expressing no exogenous HA-IκBα (lanes 1-5), low level of HA-IκBα (lanes 6-10) or high level HA-IκBα (lanes 11-15) were tested for their ability to retard a κB probe in an EMSA after various stimulation. The asynchronous stably transfected HeLa cells were either non-treated (lanes 1, 6, 11), treated by TNFα for 30 min (200 U/ mL) (lanes 2, 7, 12) or treated with CPT (10 µM) for the indicated length of time (lanes 3-5, 8-10, 13-15).

Lower panel: Nuclear extracts derived from clonal populations expressing no exogenous HA-IκBα (lanes 1-5), low level of mutated HA-IκBα (S32,36A) (lanes 6-10) or high level of HA-IκBα (S32,36) (lanes 11-15) were analyzed after TNFα or CPT stimulations as described above.

C) *S32 and S36 are required for CPT-induced degradation of IκBα*

Top panels: HeLa cells with low level expression of wild-type HA-IκBα (left panel) or high level expression of HA-IκBα (right panel) were treated by TNFα (200 U/ mL) for 30 min or by CTP (10 µM) for 1, 2 or 3 hrs as indicated. Cytoplasmic extracts were analyzed by immunoblotting; 10 µg were analyzed on the left panel and exceptionally only 1 µg on the right panel as the level of overexpression of the exogenous HA-IκBα was very high. HA-IκBα and P-HA-IκBα are indicated.

Bottom panels: HeLa cells with low level expression of HA-IκBα (S32,36A) (left panel) or high level expression of HA-IκBα (S32,S36A) (right panel) were treated by TNF-α (200 U/ mL) for 30 min or by CTP (10 µM) for 1, 2 or 3 hrs as indicated. 10 µg cytoplasmic extracts were loaded on both panels.

Fig. 5. *Importance of the 26S proteasome in the signal transduction*

A). *ALLN blocks the CPT related NF-κB activation.*

Synchronized HeLa cells were incubated with ALLN (100 µM) for 45 min (lanes 3, 4, 6) or left untreated (lanes 1, 2, 5) then subsequently treated either with TNFα (1000 U/ mL) for 30 min (lanes 2, 3) or CPT (10 µM) for 2 hours (lanes 5, 6) or left untreated (lanes 1, 4). Nuclear extracts (5 µg) prepared from these cells were tested for their ability to retard a [^{32}P]-radiolabeled probe containing the κB consensus sequence (0.2 ng). The position of the specific protein/DNA complexes and non specific complexes are indicated by sp and nsp respectively.

G) *Participation of the proteasome 26S.*

Upper panel: The presence of IκBα and P-IκBα was followed by immunoblotting of cytoplasmic extracts prepared in presence of a cocktail of phosphatase and protease inhibitors. The proteins (20 µg) were separated on a long 12 % SDS polyacrylamide gel to optimize the separation of IκBα and P-IκBα. The position of both IκBα and P-IκBα are indicated.

Middle and Lower panels: The presence of IκBα and P-IκBα was monitored in total cellular extracts derived from S phase cells treated with 10 µg/ mL Lactacystin for 45 min (lanes 3, 4 and 6 upper panel) or 25 µg/ mL E64 d for 45 min (lanes 3, 4 and 6 lower panel) prior to incubation with 1000 U/ mL TNFα for 30 min (lanes 2, 3) or 10 µg/ mL CPT for 2 hours (lanes 5, 6). The immunoblots were probed with anti-IκBα antibodies.

Fig. 6. *Dominant negative NIK mutant blocks NF-κB activation by CPT.*

A) HeLa cells were plated in 6 well tissue culture dishes. Following an overnight incubation, the cells were co-transfected with the κB reporter plasmid (200 ng) and the indicated amount of the vector expressing the catalytically inactive NIK (K429,430A). Decreasing amounts of carrier vector were added to maintain the DNA load constant. Six and a half hours after the transfection, the media was removed and fresh media containing TNFα (200 U/ mL) or CPT (3 µM) was added. Twelve hours later the cells were lyzed. The luciferase activity was reported to µg protein and presented as a relative fold induction to the basal level measured in unstimulated cells. Error bars represent sample standard deviation.

B) Same as in A except that the cells were transfected with increasing amounts of catalytically inactive MEKK1 (D1369A).

C) *Catalytically inactive NIK interferes with the activation of the IKK.*

Cells in 25 cm^2 culture flasks in process of synchronization were transfected with 4 µg of the carrier vector (lanes 1 and 2) or the vector expressing dnMEKK1 (lane 3) or the vector expressing dnNIK (lane 4). Four hours after the release of the thymidine block and 24 hours after the transfection, CPT (10 µM) was added in the cell media. After 80 min incubation, cytoplasmic extracts were prepared in presence of phosphatase and protease inhibitors. 100 µg of proteins were immunoprecipitated with anti-IKKα antibody and the IKK kinase activity of the immunoprecipitated proteins tested on GST-IκBα.

Fig. 7. *NF-κB inhibition increases cell killing by CPT.*

Different clones expressing either no exogenous HA-IκBα (filled diamond, dashed lines), low level HA-IκBα (open square), high level HA- IκBα (closed square), low level HA-IκBα (S32,36A) (open triangle), or high level HA-IκBα (S32,36) (closed triangle) were left untreated or were incubated for 48 hours with increasing concentrations of CPT (0.1-1 µM). Cell viability was estimated with WST1. Data points are means of three different experiments each of them done with triplicates.

References

1. Liu LF, Duann P, Lin CT, D'Arpa P, and Wu J. Mechanism of action of camptothecin. Ann.N.Y.Acad.Sci. 1996;803:44-49.

2. Pommier Y, Pourquier P, Fan Y, and Strumberg D. Mechanism of action of eukaryotic DNA topoisomerase I and drugs targeted to the enzyme. Biochim. Biophys. Acta 1998;1400:83-105.

3. Avemann K, Knippers R, Koller T, and Sogo JM. Camptothecin, a specific inhibitor of type I DNA topoisomerase, induces DNA breakage at replication forks. Mol.Cell Biol. 1988;8:3026-3034.

4. Ryan AJ, Squires S, Strutt HL, and Johnson RT. Camptothecin cytotoxicity in mammalian cells is associated with the induction of persistent double strand breaks in replicating DNA. Nucleic Acids Res. 1991;19:3295-3300.

5. Strumberg D, Pilon AA, Smith M, Hickey R, Malkas L, and Pommier Y. Conversion of topoisomerase I cleavage complexes on the leading strand of ribosomal DNA into 5'-phosphorylated DNA double-strand breaks by replication runoff. Mol.Cell Biol. 2000;20:3977-3987.

6. Darzynkiewicz Z, Bruno S, Del Bino G, and Traganos F. The cell cycle effects of camptothecin. Ann.N.Y.Acad.Sci. 1996;803:93-100.

7. Larsen AK and Skladanowski A. Cellular resistance to topoisomerase-targeted drugs: from drug uptake to cell death. Biochim.Biophys.Acta 1998;1400:257-274.

8. Kaufmann SH. Cell death induced by topoisomerase-targeted drugs: more questions than answers. Biochim.Biophys.Acta 1998;1400:195-211.

9. Wang Y, Perrault AR, and Iliakis G. Down-regulation of DNA replication in extracts of camptothecin-treated cells: activation of an S-phase checkpoint? Cancer Res. 1997;57: 1654-1659.

10. Falk SJ and Smith PJ. DNA damaging and cell cycle effects of the topoisomerase I poison camptothecin in irradiated human cells. Int.J.Radiat.Biol. 1992;61:749-757.

11. Johnson RT, Gotoh E, Mullinger AM, Ryan AJ, Shiloh Y, Ziv Y, and Squires S. Targeting double-strand breaks to replicating DNA identifies a subpathway of DSB repair that is defective in ataxia-telangiectasia cells. Biochem.Biophys.Res.Commun. 1999;261:317-325.

12. Kraakman-van der Zwet M, Overkamp WJ, Friedl AA, Klein B, Verhaegh GW, Jaspers NG, Midro AT, Eckardt-Schupp F, Lohman PH, and Zdzienicka MZ. Immortalization and characterization of Nijmegen Breakage syndrome fibroblasts. Mutat.Res. 1999;434: 17-27.

13. Piret B and Piette J. Topoisomerase poisons activate the transcription factor NF-kappaB in ACH-2 and CEM cells. Nucleic Acids Res. 1996;24:4242-4248.

14. Piret B, Schoonbroodt S, and Piette J. The ATM protein is required for sustained activation of NF-kappaB following DNA damage. Oncogene 1999;18:2261-2271.

15. Huang TT, Wuerzberger-Davis SM, Seufzer BJ, Shumway SD, Kurama T, Boothman DA, and Miyamoto S. NF-kappaB activation by camptothecin. A linkage between nuclear DNA damage and cytoplasmic signaling events. J.Biol.Chem. 2000;275:9501-9509.

16. Ghosh S, May MJ, and Kopp EB. NF-kappa B and Rel proteins: evolutionarily conserved mediators of immune responses. Annu.Rev.Immunol. 1998;16:225-260.

17. Li N and Karin M. Is NF-kappaB the sensor of oxidative stress? FASEB J. 1999;13:1137-1143.

18. Schoonbroodt S, Ferreira V, Best-Belpomme M, Boelaert JR, Legrand-Poels S, Korner M, and Piette J. Crucial role of the amino-terminal tyrosine residue 42 and the carboxyl-terminal PEST domain of I kappa B alpha in NF-kappa B activation by an oxidative stress. J.Immunol. 2000;164: 4292-4300.

19. Guttridge DC, Albanese C, Reuther JY, Pestell RG, and Baldwin AS. NF-kappaB controls cell growth and differentiation through transcriptional regulation of cyclin D1. Mol.Cell Biol. 1999;19:5785-5799.

20. Hinz M, Krappmann D, Eichten A, Heder A, Scheidereit C, and Strauss M. NF-kappaB function in growth control: regulation of cyclin D1 expression and G0/G1-to-S-phase transition. Mol.Cell Biol. 1999;19:2690-2698.

21. Mayo MW and Baldwin AS. The transcription factor NF-kappaB: control of oncogenesis and cancer therapy resistance. Biochim.Biophys.Acta 2000;1470:M55-M62, 2000.

22. Foo SY and Nolan GP. NF-kappaB to the rescue: RELs, apoptosis and cellular transformation. Trends Genet. 1999;15:229-235.

23. Bentires-Alj M, Hellin AC, Ameyar M, Chouaib S, Merville MP, and Bours V. Stable inhibition of nuclear factor kappaB in cancer cells does not increase sensitivity to cytotoxic drugs. Cancer Res. 1999;59:811-815.

24. Mercurio F and Manning AM. Multiple signals converging on NF-kappaB. Curr.Opin.Cell Biol. 1999;11:226-232.

25. Karin M. The beginning of the end: IkappaB kinase (IKK) and NF-kappaB activation. J.Biol.Chem. 1999;274:27339-27342.

26. Yamamoto Y, Yin MJ, and Gaynor RB. IkappaB kinase alpha (IKKalpha) regulation of IKKbeta kinase activity. Mol.Cell Biol. 2000;20:3655-3666.

27. Li N and Karin M. Ionizing radiation and short wavelength UV activate NF-kappaB through two distinct mechanisms. Proc.Natl.Acad.Sci.U.S.A 1998;95:13012-13017.

28. Bender K, Gottlicher M, Whiteside S, Rahmsdorf HJ, and Herrlich P. Sequential DNA damage-independent and -dependent activation of NF- kappaB by UV. EMBO J. 1998;17:5170-5181.

29. Mercurio F, Zhu H, Murray BW, Shevchenko A, Bennett BL, Li J, Young DB, Barbosa M, Mann M, Manning A, and Rao A. IKK-1 and IKK-2: cytokine-activated IkappaB kinases essential for NF- kappaB activation. Science 1997;278:860-866.

30. Cohen L, Henzel WJ, and Baeuerle PA. IKAP is a scaffold protein of the IkappaB kinase complex. Nature 1998;395:292-296.

31. Lin X, Cunningham ET, Jr., Mu Y, Geleziunas R, and Greene WC. The proto-oncogene Cot kinase participates in CD3/CD28 induction of NF- kappaB acting through the NF-kappaB-inducing kinase and IkappaB kinases. Immunity. 1999;10:271-280.

32. Malinin NL, Boldin MP, Kovalenko AV, and Wallach D. MAP3K-related kinase involved in NF-kappaB induction by TNF, CD95 and IL-1. Nature 1997;385:540-544.

33. Nemoto S, DiDonato JA, and Lin A. Coordinate regulation of IkappaB kinases by mitogen-activated protein kinase kinase kinase 1 and NF-kappaB-inducing kinase. Mol.Cell Biol. 1998;18:7336-7343.

34. Sylla BS, Hung SC, Davidson DM, Hatzivassiliou E, Malinin NL, Wallach D, Gilmore TD, Kieff E, and Mosialos G. Epstein-Barr virus-transforming protein latent infection membrane protein 1 activates transcription factor NF-kappaB through a pathway that includes the NF-kappaB-inducing kinase and the IkappaB kinases IKKalpha and IKKbeta. Proc.Natl.Acad.Sci.U.S.A 1998;95:10106-10111.

35. Yin MJ, Christerson LB, Yamamoto Y, Kwak YT, Xu S, Mercurio F, Barbosa M, Cobb MH, and Gaynor RB. HTLV-I Tax protein binds to MEKK1 to stimulate IkappaB kinase activity and NF-kappaB activation. Cell 1998;93:875-884.

36. Zamanian-Daryoush M, Mogensen TH, DiDonato JA, and Williams BR. NF-kappaB activation by double-stranded-RNA-activated protein kinase (PKR) is mediated through NF-kappaB-inducing kinase and IkappaB kinase. Mol.Cell Biol. 2000;20:1278-1290.

37. Rao PN and Johnson RT. Mammalian cell fusion: studies on the regulation of DNA synthesis and mitosis. Nature 1970;225:159-164.

38. Ling Y, West AG, Roberts EC, Lakey JH, and Sharrocks AD. Interaction of transcription factors with serum response factor. Identification of the Elk-1 binding surface. J.Biol.Chem. 1998;273:10506-10514.

39. Neumann J, Rorency C, and Russian K. A novel rapid assay for chloramphenicol acetyltransferase gene expression. Biotechniques 2001;5:444-447.

40. Supko J and Malspeis L. Pharmacokinetics of the 9-amino and 10,11-methylenedioxy derivatives of camptothecin in mice. Cancer Res. 1993;53:3062-3069.

41. Zandi E and Karin M. Bridging the gap: composition, regulation, and physiological

function of the IkappaB kinase complex. Mol.Cell Biol. 1999;19:4547-4551.

42. Han Y, Weinman S, Boldogh I, Walker RK, and Brasier AR. Tumor necrosis factor-alpha-inducible IkappaBalpha proteolysis mediated by cytosolic m-calpain. A mechanism parallel to the ubiquitin- proteasome pathway for nuclear factor-kappab activation. J.Biol.Chem. 1999;274:787-794.

43. Rock KL, Gramm C, Rothstein L, Clark K, Stein R, Dick L, Hwang D, and Goldberg AL. Inhibitors of the proteasome block the degradation of most cell proteins and the generation of peptides presented on MHC class I molecules. Cell 1994;78:761-771.

44. Sasaki T, Kishi M, Saito M, Tanaka T, Higuchi N, Kominami E, Katunuma N, and Murachi T. Inhibitory effect of di- and tripeptidyl aldehydes on calpains and cathepsins. J.Enzyme Inhib. 1990;3:195-201.

45. Beg AA and Baldwin AS. Activation of multiple NF-kappa B/Rel DNA-binding complexes by tumor necrosis factor. Oncogene 1994;9:1487-1492.

46. Chen FE and Ghosh G. Regulation of DNA binding by Rel/NF-kappaB transcription factors: structural views. Oncogene 1999;18:6845-6852.

47. Menetski JP. The structure of the nuclear factor-kappaB protein-DNA complex varies with DNA-binding site sequence. J.Biol.Chem. 2000;275:7619-7625.

48. Kunsch C, Ruben SM, and Rosen CA. Selection of optimal kappa B/Rel DNA-binding motifs: interaction of both subunits of NF-kappa B with DNA is required for transcriptional activation. Mol.Cell Biol. 1992;12:4412-4421.

49. Whiteside ST, Epinat JC, Rice NR, and Israel A. I kappa B epsilon, a novel member of the I kappa B family, controls RelA and cRel NF-kappa B activity. EMBO J. 1997;16:1413-1426.

50. Hofland K, Petersen BO, Falck J, Helin K, Jensen PB, and Sehested M. Differential cytotoxic pathways of topoisomerase I and II anticancer agents after overexpression of the E2F-1/DP-1 transcription factor complex . Clin.Cancer Res. 2000;6:1488-1497.

51. Lim DS, Kim ST, Xu B, Maser RS, Lin J, Petrini JH, and Kastan MB. ATM phosphorylates p95/nbs1 in an S-phase checkpoint pathway. Nature 2000;404:613-617.

52. Heusch M, Lin L, Geleziunas R, and Greene WC. The generation of nfkb2 p52: mechanism and efficiency. Oncogene 1999;18:6201-6208.

53. Hayashi T and Faustman D. Essential role of human leukocyte antigen-encoded proteasome subunits in NF-kappaB activation and prevention of tumor necrosis factor-alpha- induced apoptosis. J.Biol.Chem. 2000;275: 5238-5247.

54. Lin L, DeMartino GN, and Greene WC. Cotranslational biogenesis of NF-kappaB p50 by the 26S proteasome. Cell 1998;92:819-828.

55. Desai SD, Liu LF, Vazquez-Abad D, and D'Arpa P. Ubiquitin-dependent destruction of topoisomerase I is stimulated by the antitumor drug camptothecin. J.Biol.Chem. 1997;272:24159-24164.

56. Fu Q, Kim SW, Chen HX, Grill S, and Cheng YC. Degradation of topoisomerase I induced by topoisomerase I inhibitors is dependent on inhibitor structure but independent of cell death. Mol.Pharmacol. 1999;55:677-683.

57. Mao Y, Sun M, Desai SD, and Liu LF. SUMO-1 conjugation to topoisomerase I: A possible repair response to topoisomerase-mediated DNA damage. Proc.Natl.Acad.Sci. 2000;97:4046-4051.

58. Tabata M, Tabata R, Grabowski DR, Bukowski RM, Ganapathi MK, and Ganapathi R. Roles of NF-{kappa}B and 26S proteasome in apoptotic cell death induced by Topoisomerase I and II poisons in human non-small cell lung carcinoma. J.Biol.Chem. 2001;276:8029-8036.

59. Wang X, Luo H, Chen H, Duguid W, and Wu J. Role of proteasomes in T cell activation and proliferation. J.Immunol. 1998;160:788-801.

60. Sherwood SW, Kung AL, Roitelman J, Simoni RD, and Schimke RT. In vivo inhibition of cyclin B degradation and induction of cell-cycle arrest in mammalian cells by the neutral cysteine protease inhibitor N- acetylleucylleucylnorleucinal. Proc.Natl.Acad.Sci. 1993;90:3353-3357.

61. Habib AA, Chatterjee S, Park SK, Ratan RR, Lefebvre S, and Vartanian T. The epidermal growth factor receptor engages RIP (receptor interacting protein) and NIK (NF-kB inducing kinase) to activate NF-kB: Identification of a novel RTK signalosome. J.Biol.Chem. 2001;276:8865-8874.

Figure 1 A

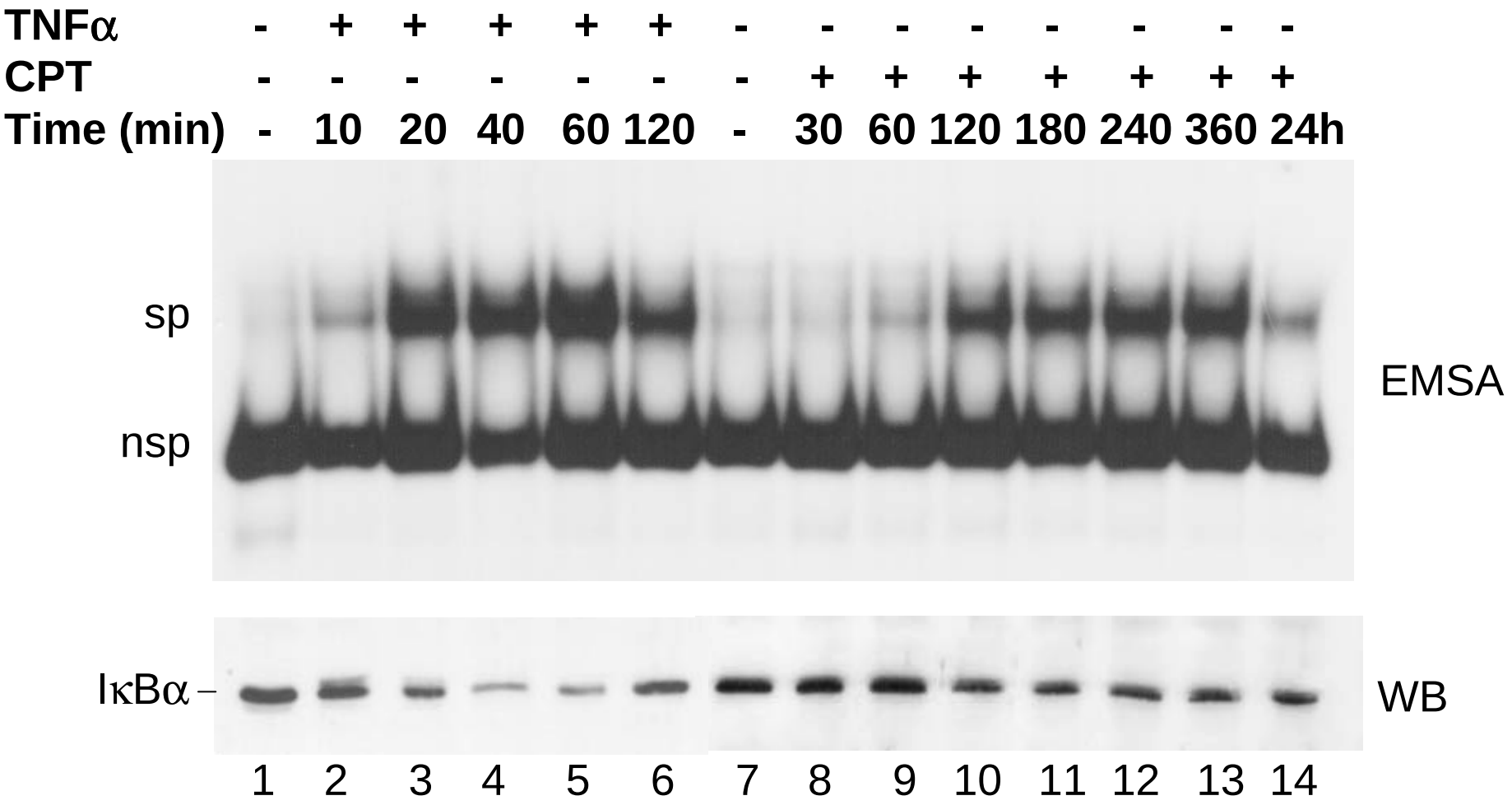
TNFα - + + + + + - - - - - - - -
CPT - - - - - - - + + + + + + +
Time (min) - 10 20 40 60 120 - 30 60 120 180 240 360 24h
sp
nsp
EMSA
IκBα
WB
1 2 3 4 5 6 7 8 9 10 11 12 13 14

Figure 1 B

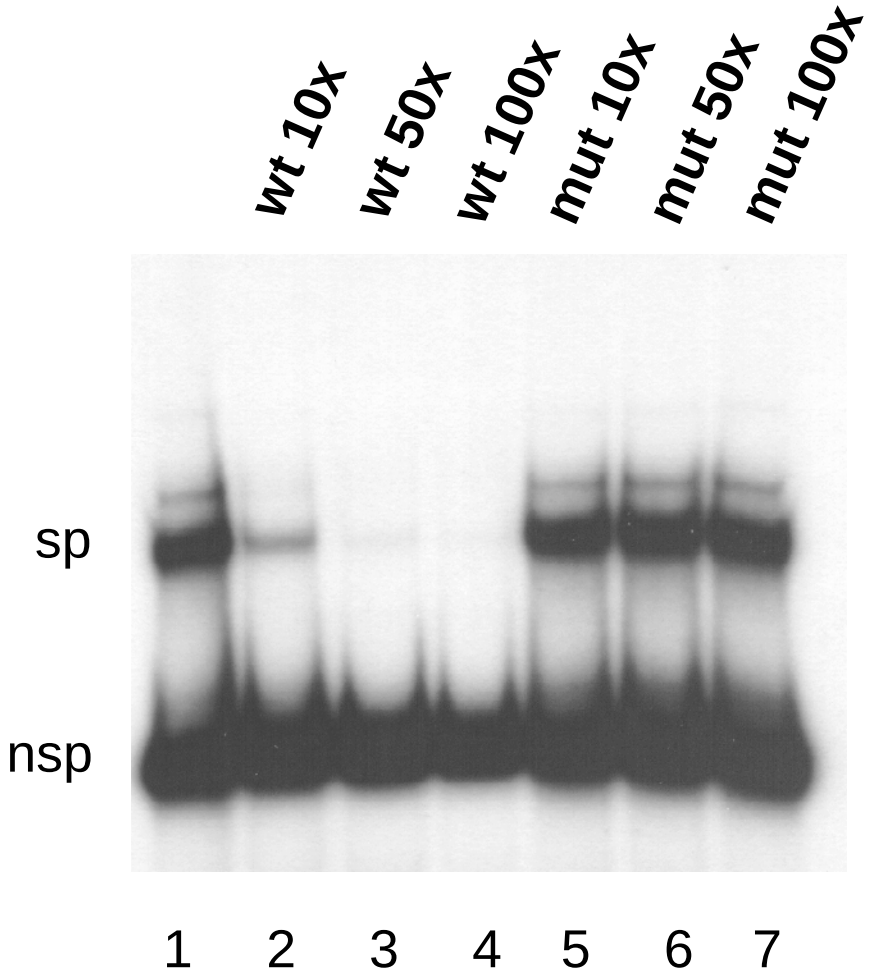

Figure 1C

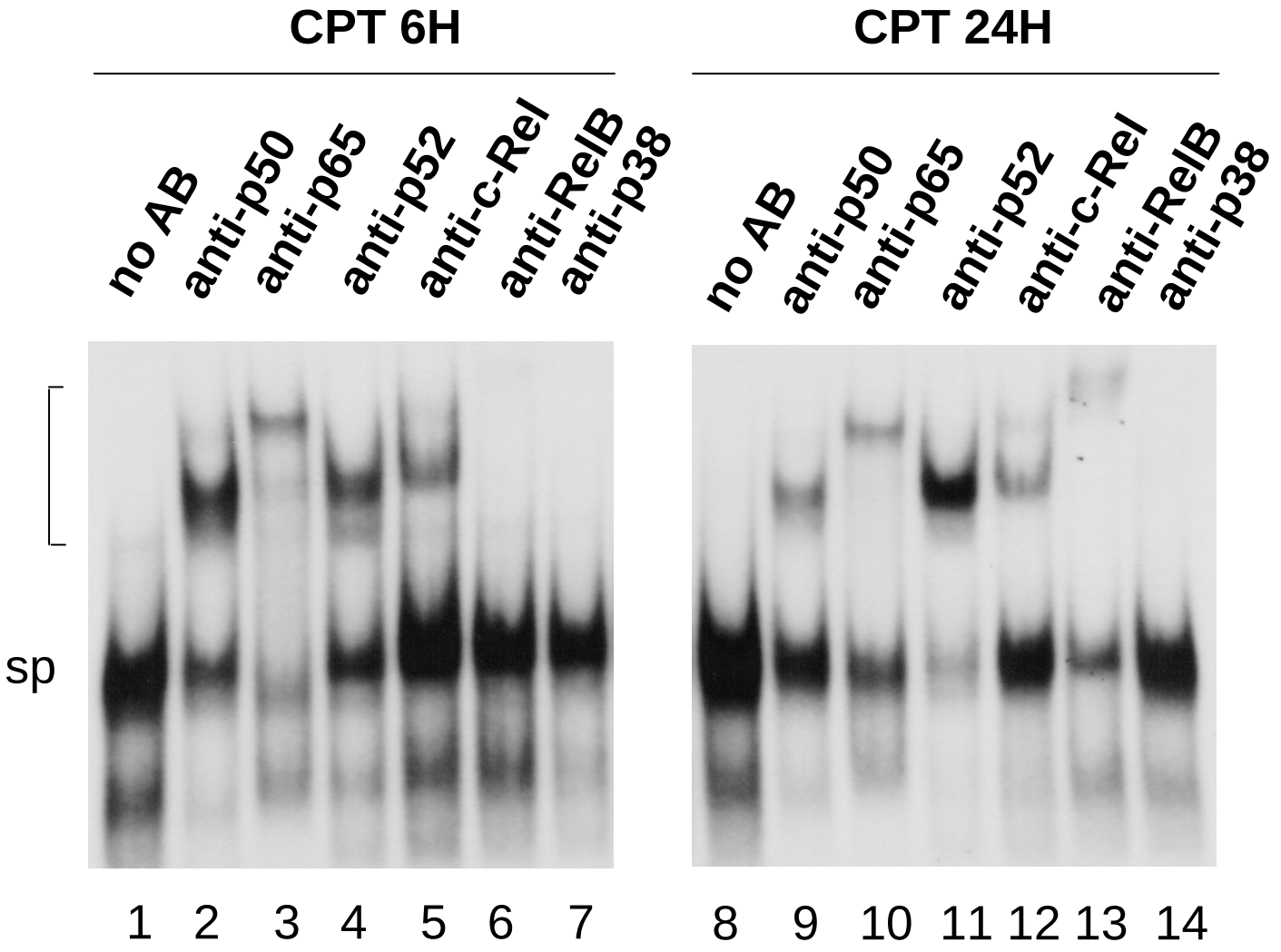
CPT 6H
CPT 24H
no AB
anti-p50
anti-p65
anti-p52
anti-c-Rel
anti-RelB
anti-p38
no AB
anti-p50
anti-p65
anti-p52
anti-c-Rel
anti-RelB
anti-p38
sp
1 2 3 4 5 6 7
8 9 10 11 12 13 14

Figure 2 A

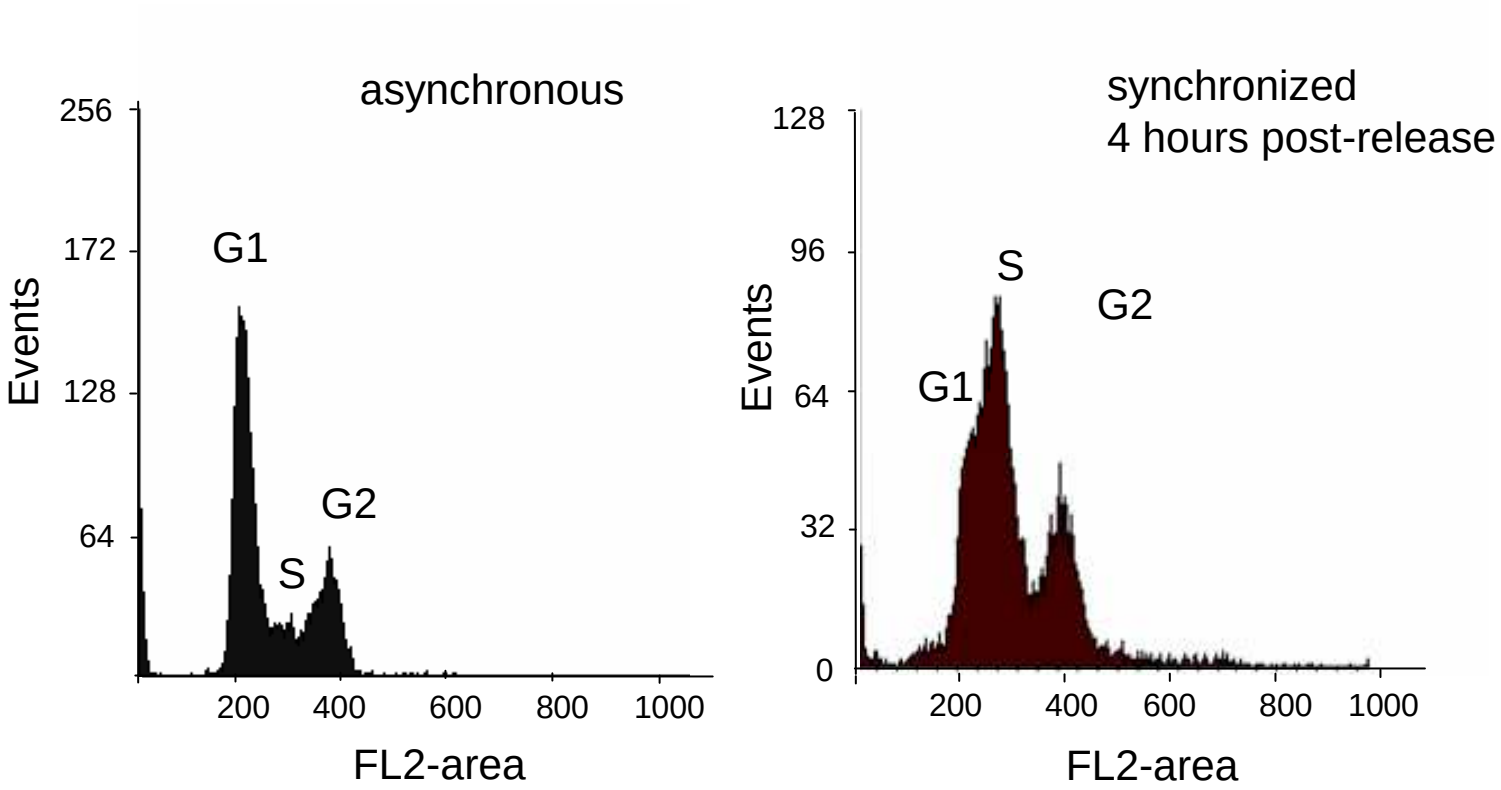
asynchronous
256
172
128
64
Events
G1
S
G2
200
400
600
800
1000
FL2-area
synchronized
4 hours post-release
128
96
64
32
0
Events
S
G2
G1
200
400
600
800
1000
FL2-area

Figure 2 B

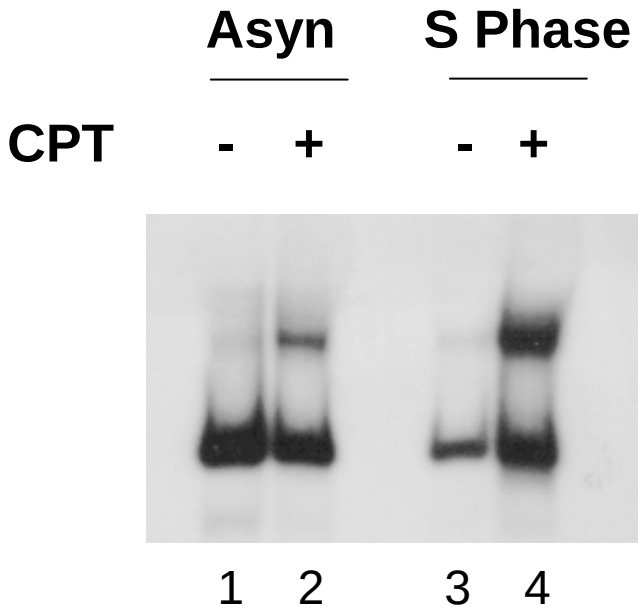

Figure 2 C

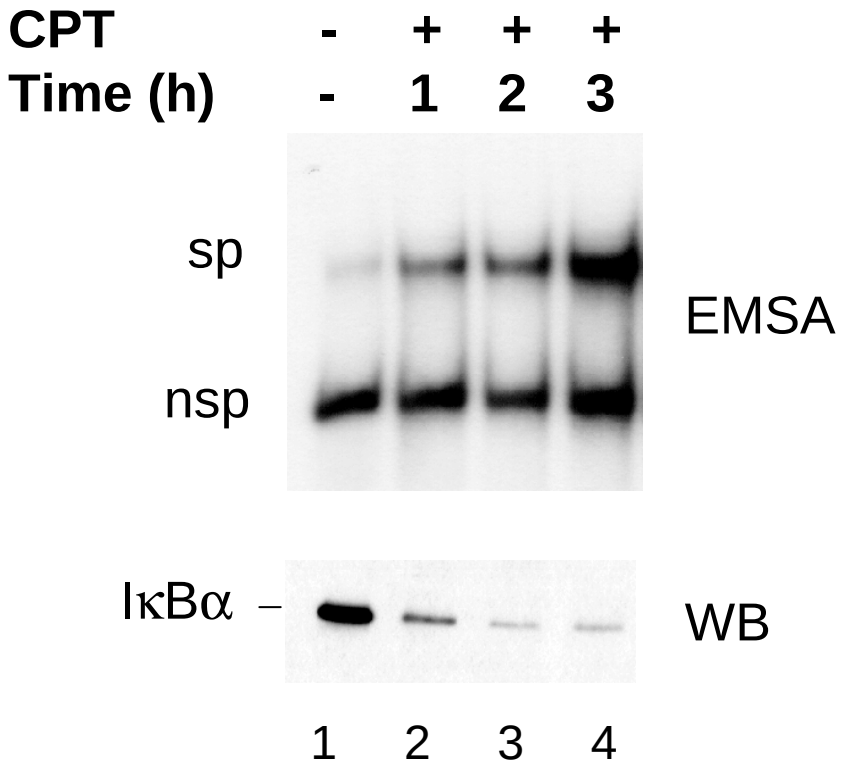

Figure 2 D

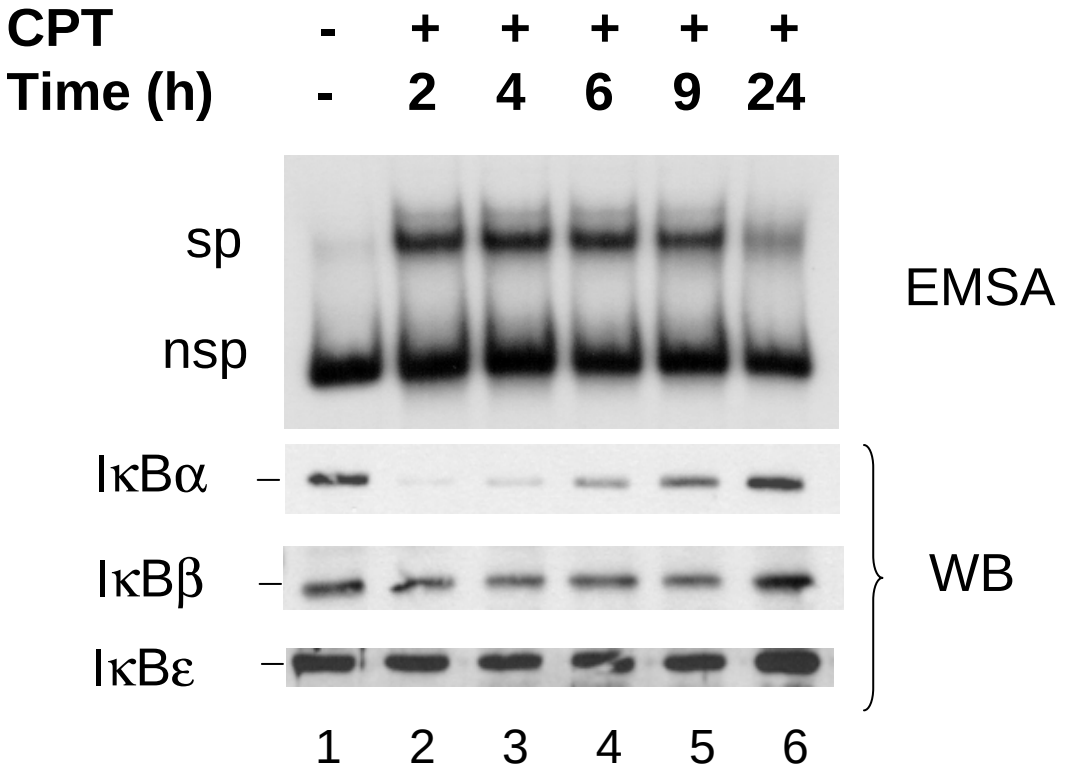

Figure 2 E

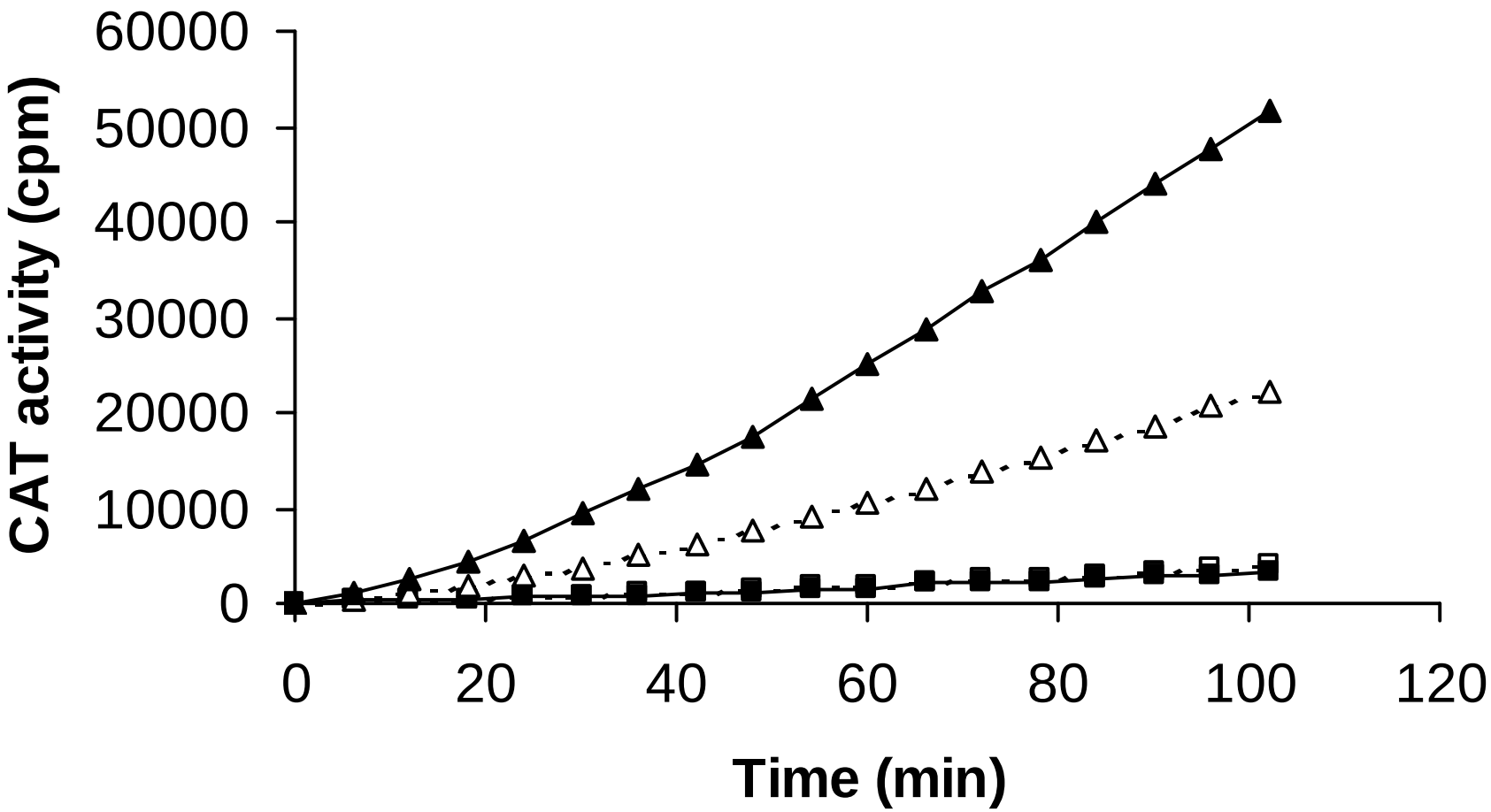
60000
50000
40000
30000
20000
10000
0
CAT activity (cpm)
0
20
40
60
80
100
120
Time (min)

Figure 3 A

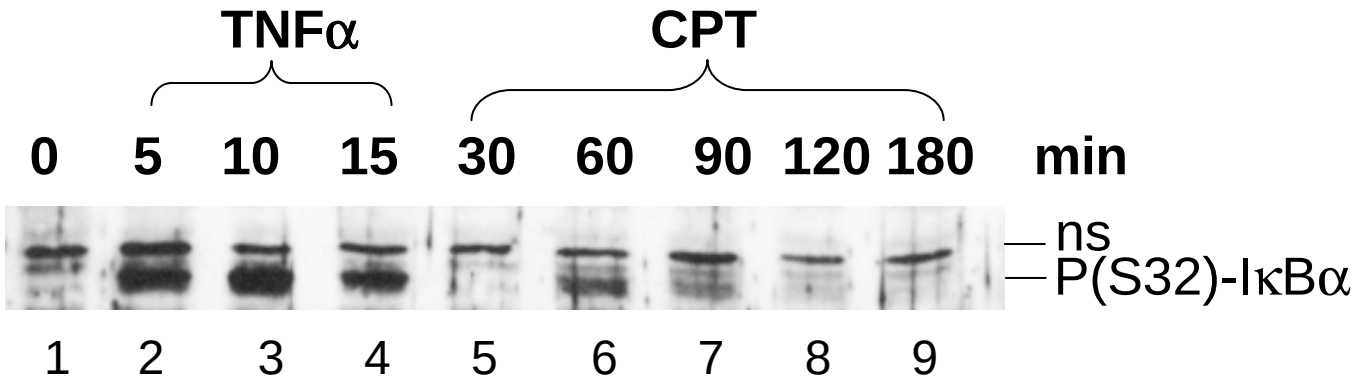

Figure 3 B

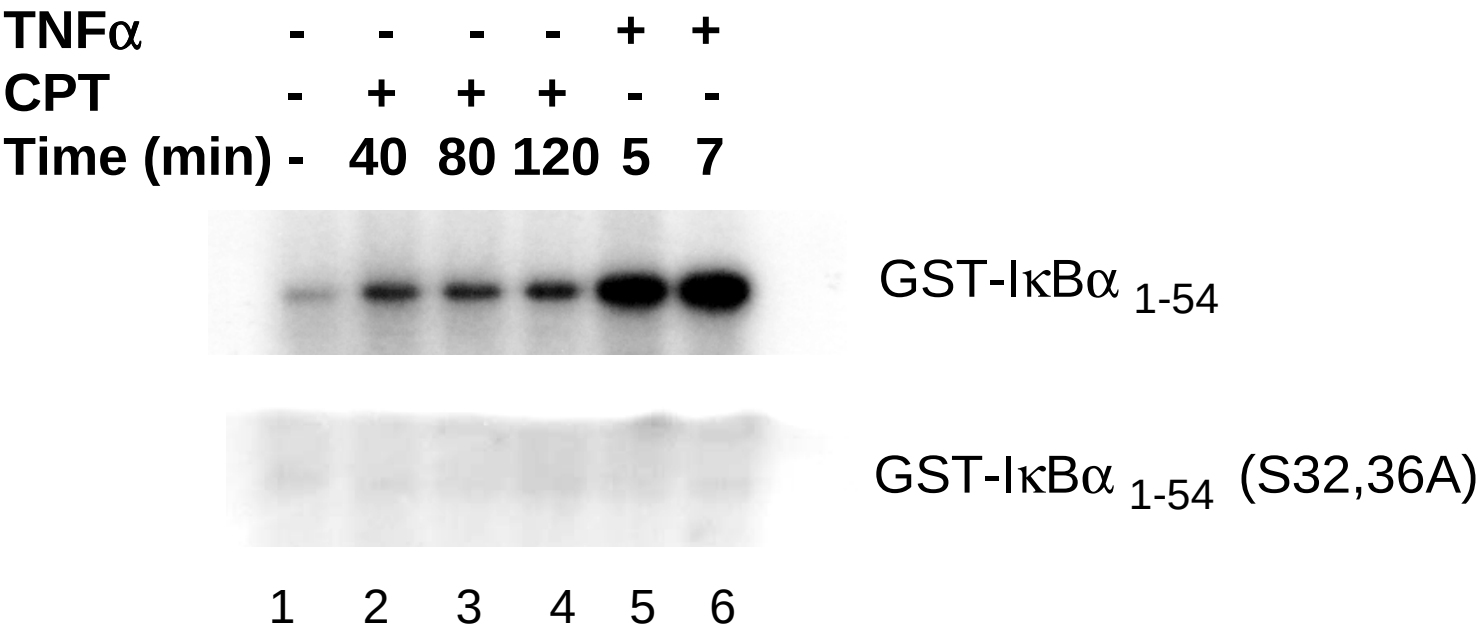
TNFα - - - - + +
CPT - + + + - -
Time (min) - 40 80 120 5 7
GST-IκBα 1-54
GST-IκBα 1-54 (S32,36A)
1 2 3 4 5 6

Figure 4 A

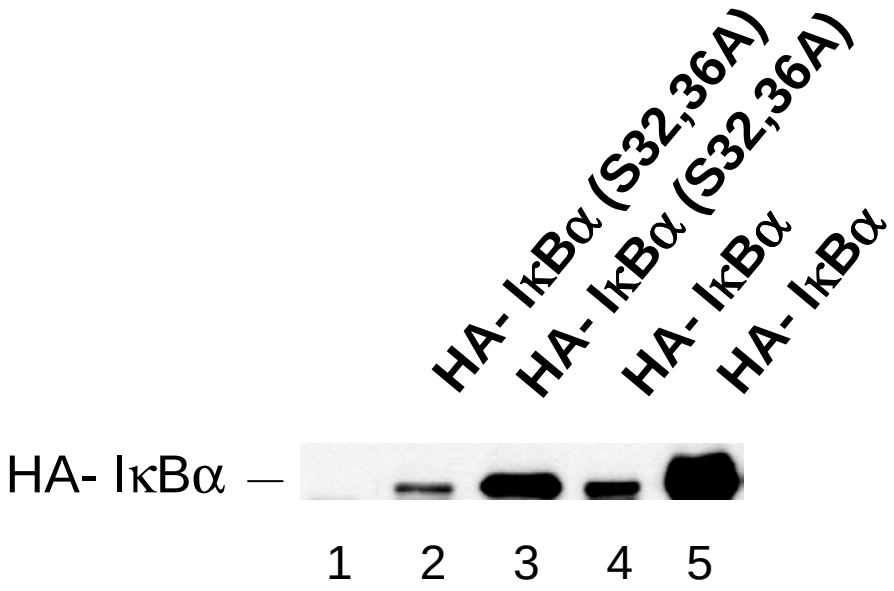

Figure 4B

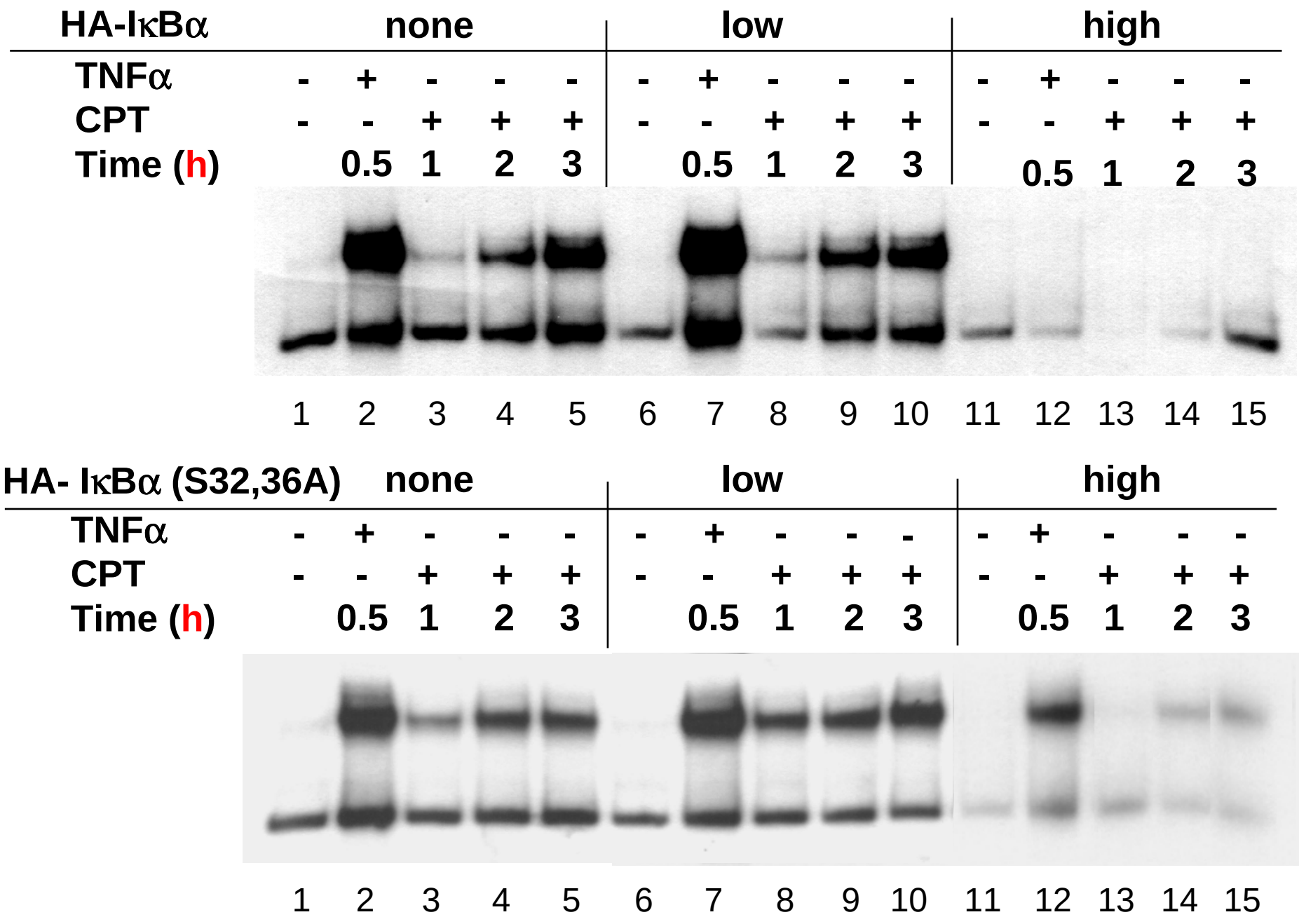
HA-IκBα
none
low
high
TNFα - + - - - - + - - - - + - - -
CPT - - + + + - - + + + - - + + +
Time (h) 0.5 1 2 3 0.5 1 2 3 0.5 1 2 3
1 2 3 4 5 6 7 8 9 10 11 12 13 14 15
HA- IκBα (S32,36A)
none
low
high
TNFα - + - - - - + - - - - + - - -
CPT - - + + + - - + + + - - + + +
Time (h) 0.5 1 2 3 0.5 1 2 3 0.5 1 2 3
1 2 3 4 5 6 7 8 9 10 11 12 13 14 15

Figure 4 C

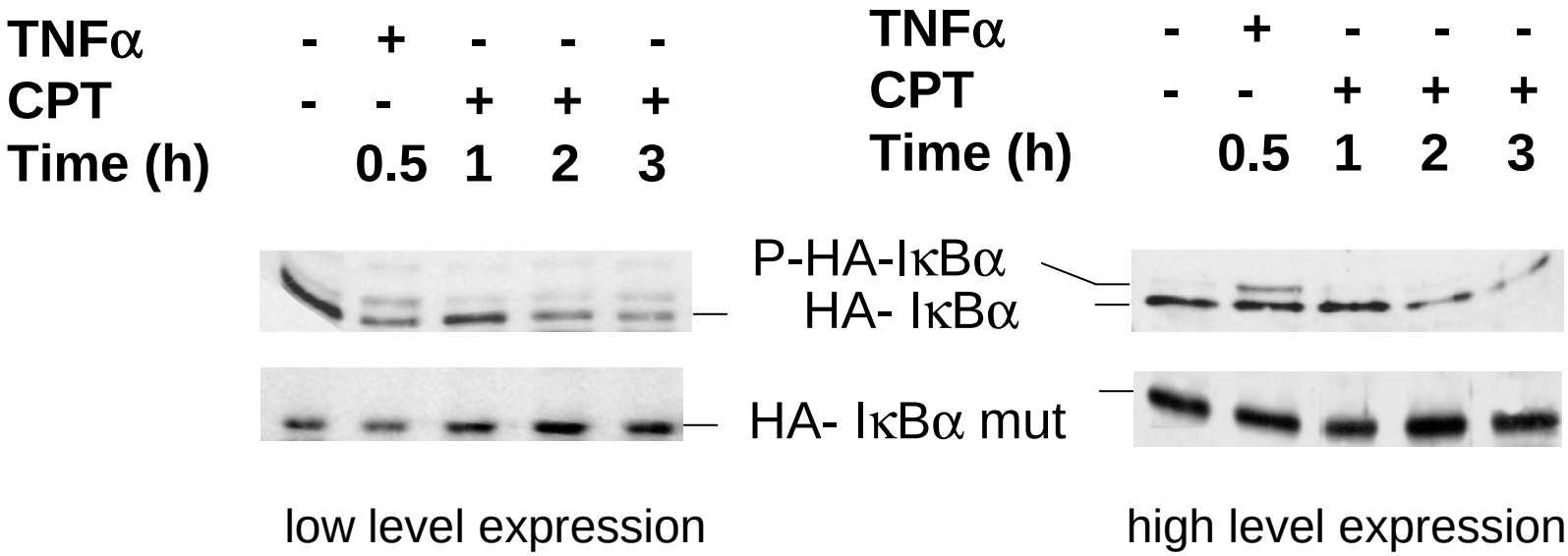
TNFα - + - - -
CPT - - + + +
Time (h) 0.5 1 2 3
TNFα - + - - -
CPT - - + + +
Time (h) 0.5 1 2 3
P-HA-IκBα
HA- IκBα
HA- IκBα mut
low level expression
high level expression

Figure 5 A

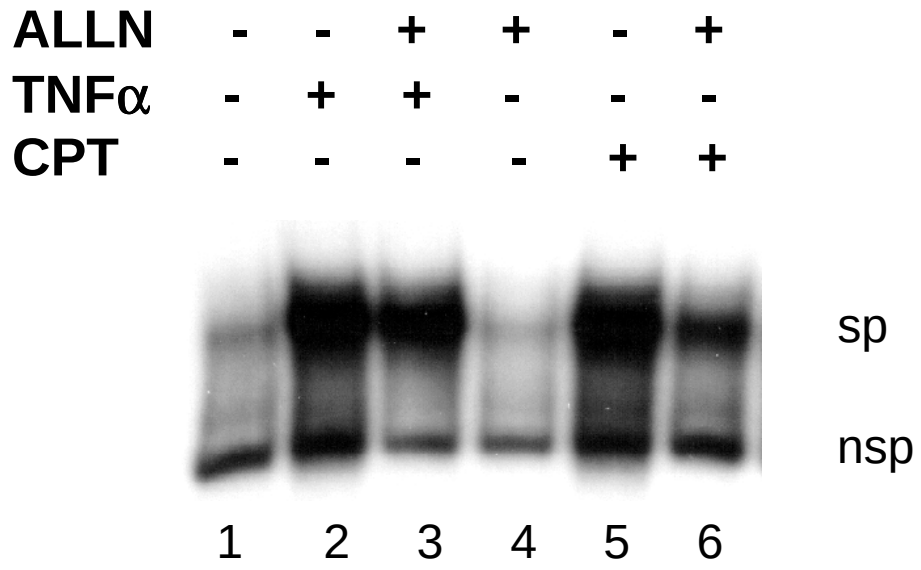

Figure 6 B

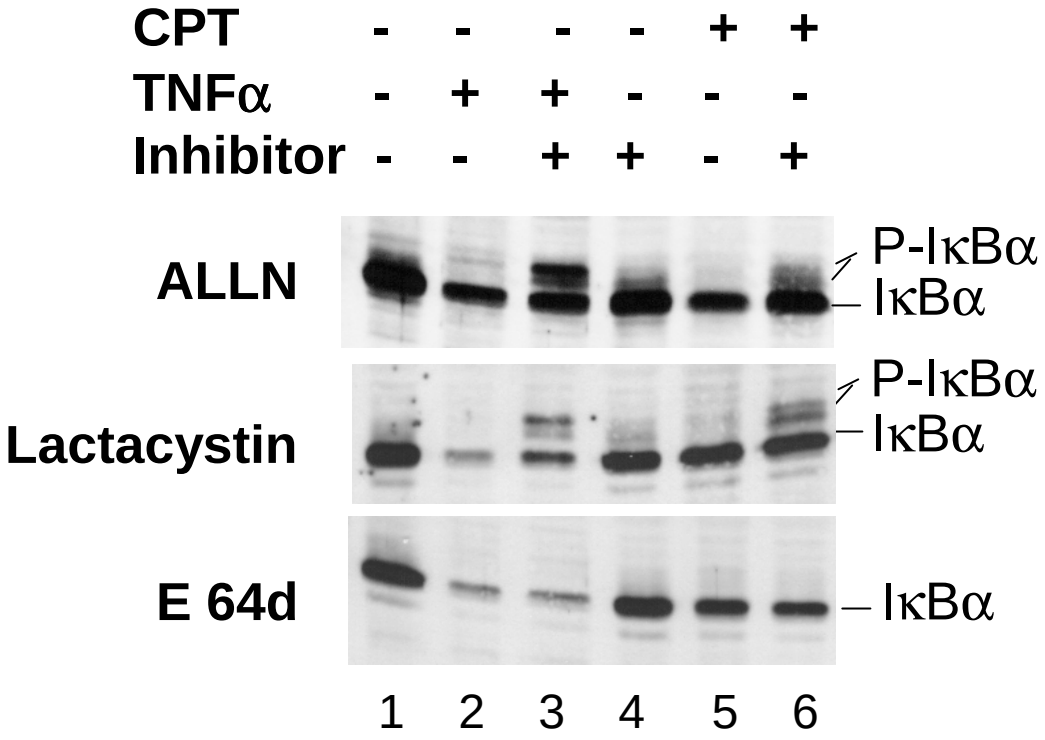
CPT - - - - + +
TNFα - + + - - -
Inhibitor - - + + - +
ALLN
P-IκBα
IκBα
Lactacystin
P-IκBα
IκBα
E 64d
IκBα
1 2 3 4 5 6

Figure 6 A

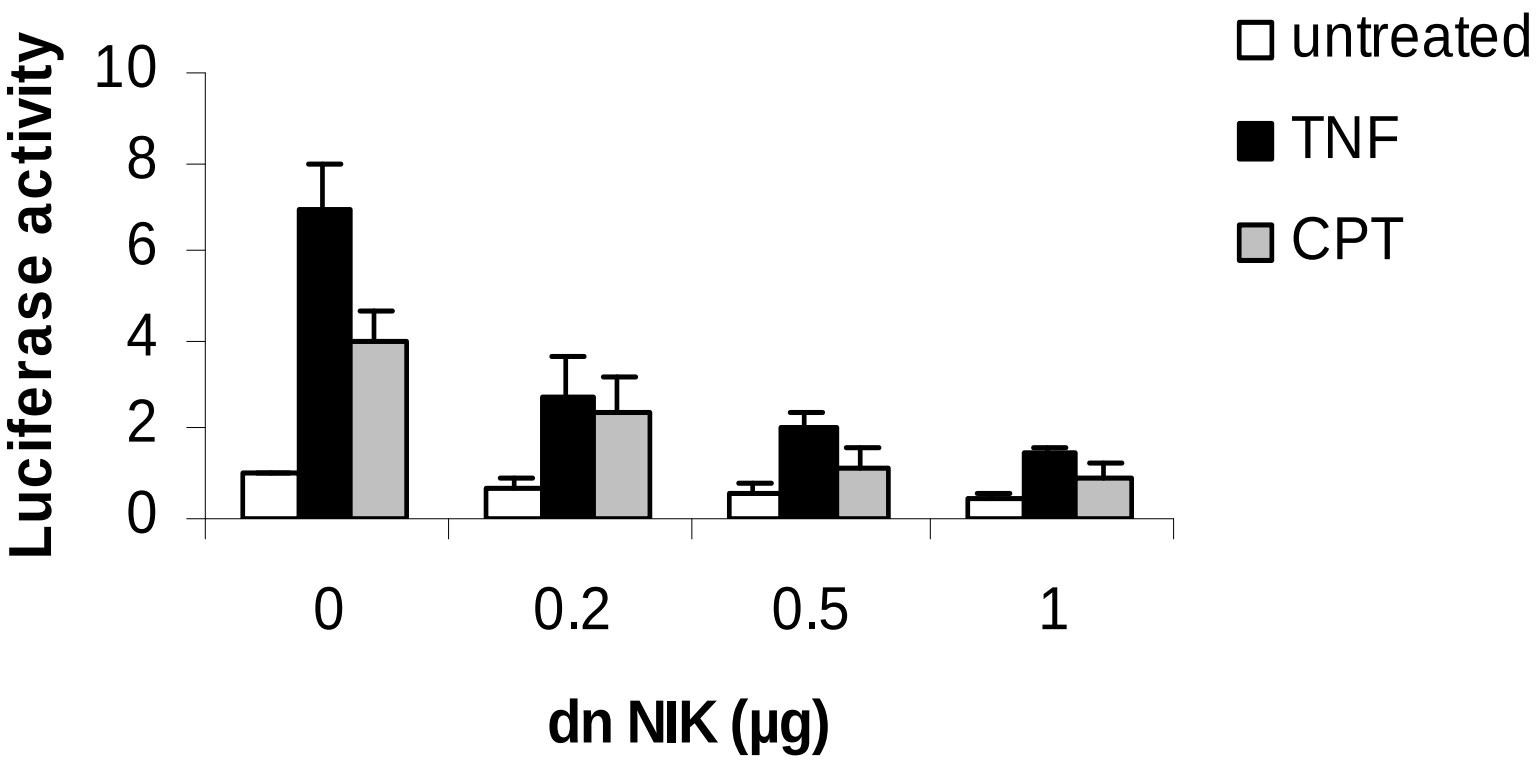
Luciferase activity
10
8
6
4
2
0
0
0.2
0.5
1
dn NIK (µg)
untreated
TNF
CPT

Figure 7 B

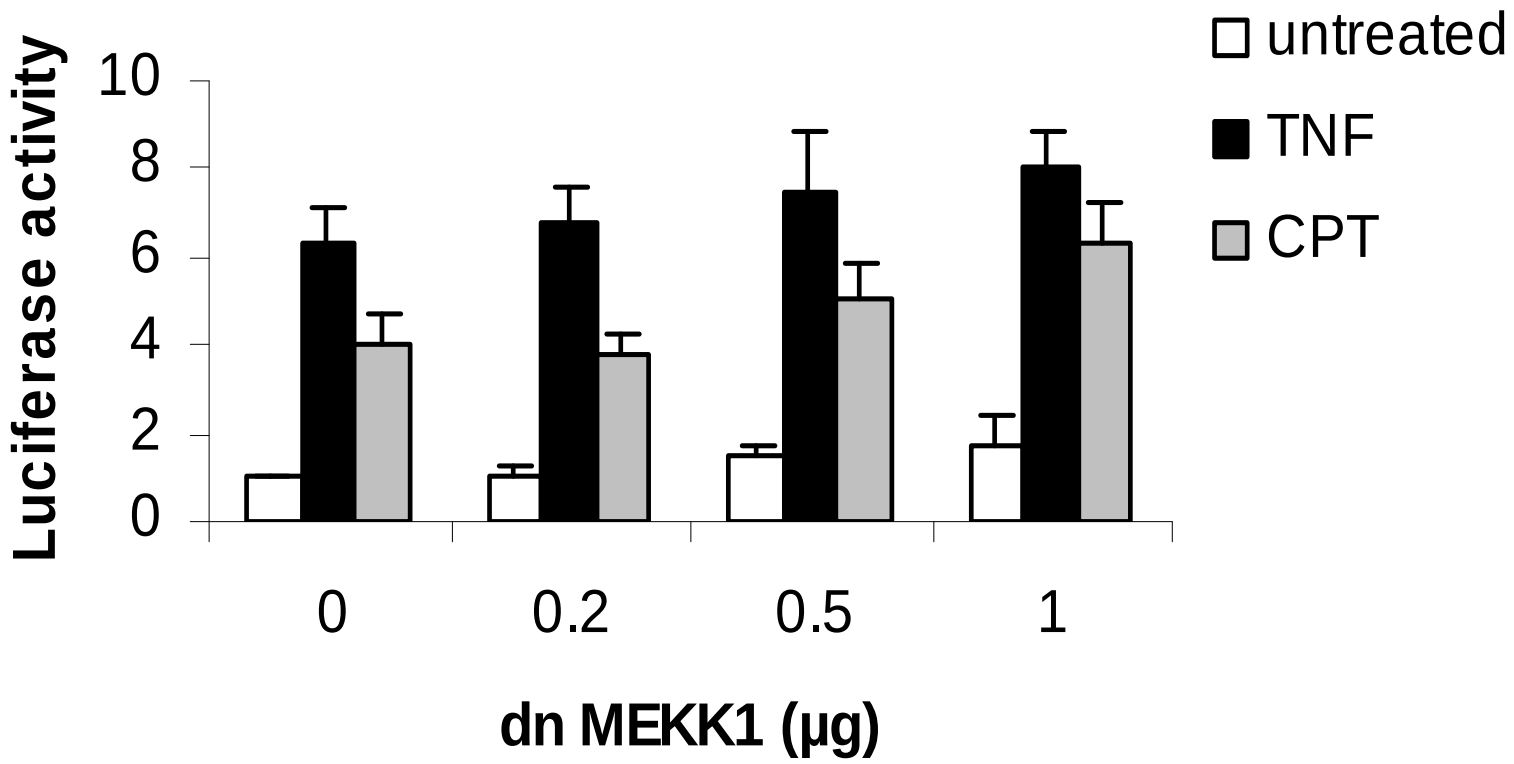
Luciferase activity
10
8
6
4
2
0
0
0.2
0.5
1
dn MEKK1 (µg)
untreated
TNF
CPT

Figure 6 C

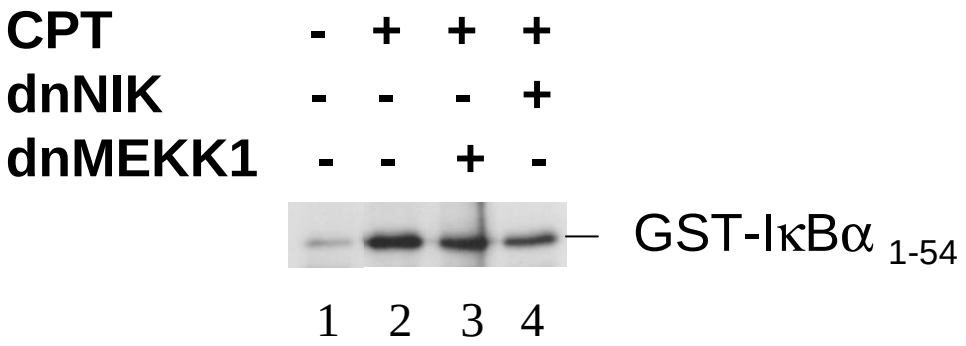

Figure 7

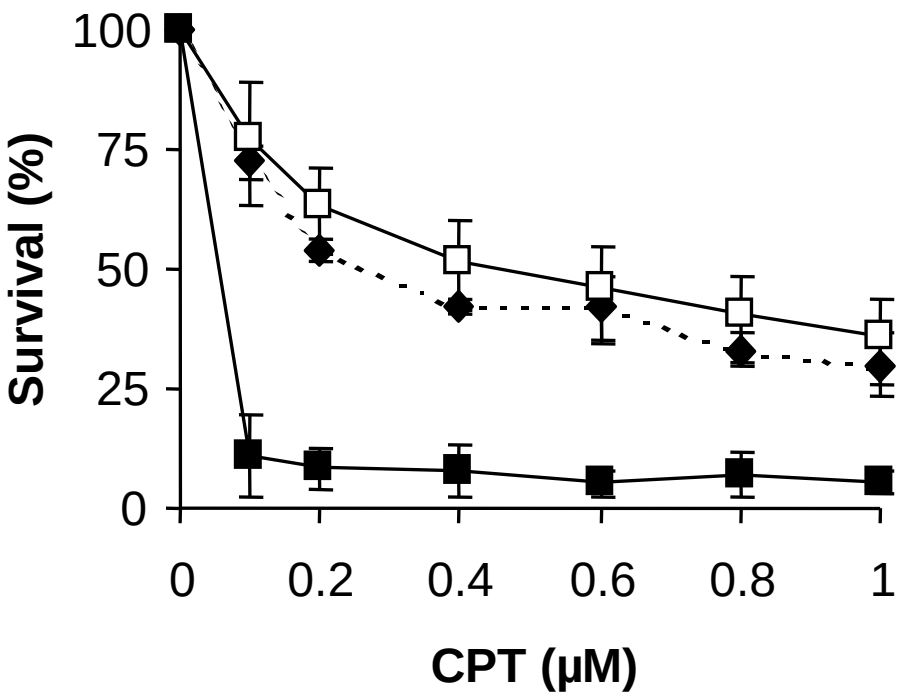
100
75
50
25
0
Survival (%)
0
0.2
0.4
0.6
0.8
1
CPT (μM)

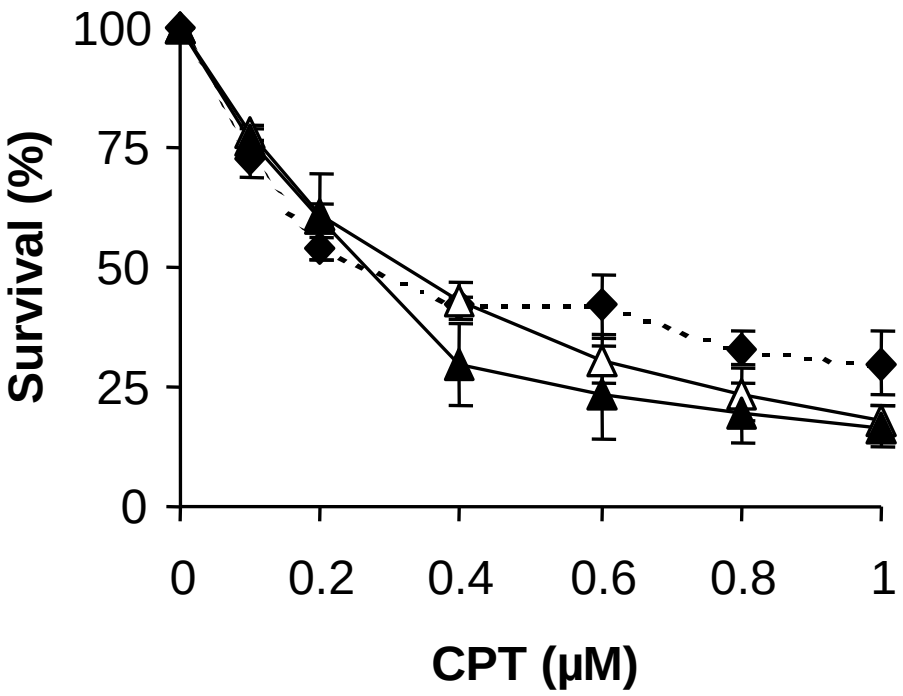
100
75
50
25
0
Survival (%)
0
0.2
0.4
0.6
0.8
1
CPT (μM)